Influence of microencapsulated Phase Change Materials (PCMs) on the properties of polymer modified cementitious repair mortar

Rogiros Illampas, Ioannis Rigopoulos, Ioannis Ioannou

PII: S2352-7102(21)00184-4

DOI: https://doi.org/10.1016/j.jobe.2021.102328

Reference: JOBE 102328

To appear in: *Journal of Building Engineering*

Received Date: 16 November 2020

Revised Date: 8 February 2021

Accepted Date: 20 February 2021

Please cite this article as: R. Illampas, I. I. Ioannou, Influence of microencapsulated Phase Change Materials (PCMs) on the properties of polymer modified cementitious repair mortar, *Journal of Building Engineering*, https://doi.org/10.1016/j.jobe.2021.102328.

CRediT author statement

Rogiros Illampas: Conceptualization, Methodology, Investigation, Validation, Formal Analysis, Visualization, Writing - Original Draft. **Ioannis Rigopoulos:** Conceptualization, Methodology, Investigation, Validation, Writing - Original Draft. **Ioannis Ioannou**: Conceptualization, Methodology, Resources, Validation, Writing - Review & Editing, Supervision, Project administration, Funding acquisition.

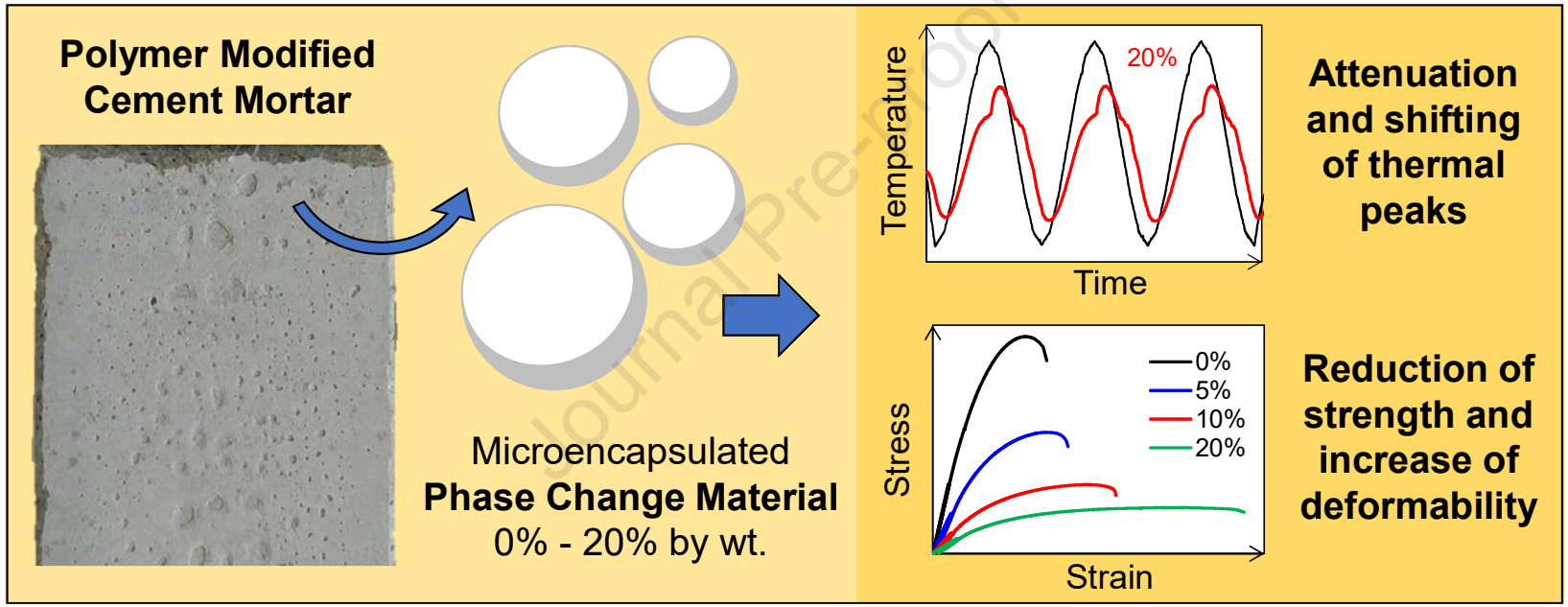

Influence of microencapsulated Phase Change Materials (PCMs) on the properties of polymer modified cementitious repair mortar

Rogiros Illampas[1], Ioannis Rigopoulos[1], Ioannis Ioannou[1,*]

[1] Department of Civil and Environmental Engineering, University of Cyprus, 75 Kallipoleos str., P.O. Box 20537, 1678 Nicosia, Cyprus

Phone: +357 22892257

Fax: +357 22895318

Emails: rilamp01@ucy.ac.cy ; rigopoulos.ioannis@ucy.ac.cy ; ioannis@ucy.ac.cy

URL: http://www.ucy.ac.cy/cee/en/

[*] Corresponding author

Keywords

- Phase Change Material (PCM)
- Cement mortar
- Physical and mechanical properties
- Pore structure
- Stress-strain behavior
- Thermal properties

Abstract

Microencapsulated Phase Change Materials (PCMs) can be directly incorporated into mortars to enhance their thermal performance. In this study, the addition of a commercial microencapsulated PCM in a polymer modified cement mortar was investigated, aiming at the development of a thermally efficient repair composite that may be used, along with textile reinforcement, for the structural and energy retrofitting of existing building envelopes. The effect of incorporating this PCM into the reference mortar at percentages ranging from 5% to 20% by wt. of solid constituents was thoroughly evaluated by assessing the physico-mechanical and thermal properties of the hardened end-product. Emphasis was placed on specific operational characteristics associated with the intended use of the modified mortar, such as its stress-strain behavior and temperature regulating efficiency. The results show a substantial drop in the mechanical properties of the composite with PCM addition, as well as an increase in its porosity and deformation capacity. In terms of thermal performance, the microencapsulated PCM contributed towards the attenuation and time shifting of temperature peaks. At dosages ≤ 20% by wt., it was thus possible to obtain mortars with favorable thermal characteristics, without compromising their physico-mechanical behavior to a degree that would preclude repair/strengthening applications.

1 Introduction

Improving the energy efficiency of buildings is one of the major challenges towards environmental sustainability. The recently updated EU policy framework for energy performance in buildings (EU 2018/844 [**1**]) and the increasing relevant requirements set by national building codes and regulations, promote the renovation and energy upgrading of existing buildings. Given the aging building stock encountered in most countries and the high seismicity of many regions, however, energy upgrading alone cannot be considered a viable solution, unless measures to ensure adequate structural performance are also taken. Studies ([**2**], [**3**], [**4**]) have shown that concurrent energy retrofitting and strengthening of building envelopes is feasible via the application of Textile Reinforced Mortar (TRM) structural overlays combined with thermal insulation.

Traditional building insulation materials are normally used in thick or multiple layers in order to achieve higher thermal resistances. This results in complex building details, an adverse net-to-gross floor area and possibly heavier load-bearing structures [**5**]. Advanced, sustainable and better performing insulation materials are therefore needed.

Phase Change Materials (PCMs) can function as latent heat storage media ([**6**], [**7**]). They can absorb energy while being heated, by changing phase from solid to liquid state. When the ambient temperature drops, they re-solidify, releasing the energy previously absorbed. The endothermic and exothermic processes which take place during the phase change cycle can contribute towards attenuating temperature fluctuations in building spaces [**8**].

PCMs can be encapsulated within chemically and physically stable shells, 1-1000 μm in size, using various techniques (e.g. polymerization, coacervation, spray drying, pan coating etc.) [**9**]. Direct integration of PCM microcapsules into cementitious mortars is a widely used technique [**10**], which exhibits obvious advantages in terms of practicality and cost-efficiency ([**11**], [**12**], [**13**]). However, the efficiency of this technique is influenced by the durability of the encapsulation shell. Capsule breakage during mixing and/or casting may cause PCM leakage, which can negatively affect the performance of the end-product. In

addition, the large surface area of the fine PCM particles and/or the use of absorbent encapsulation shells can increase the demand for mixing water to maintain adequate consistency at fresh state [**14**]. This, inevitably, negatively affects the mechanical properties of the hardened composite end-product. Table 1 presents data from the literature showing the effect of microencapsulated PCM addition on the physico-mechanical and thermal properties of cement-based mortars.

Table 1. Properties of cement-based mortars incorporating microencapsulated PCMs. In each case, the properties of the reference mixtures not containing PCM (Ref.) are reported, along with the corresponding properties of the PCM-modified mixtures (PCM).

Study	Type of application	PCM incorporation	f_c (MPa)	$f_{t,b}$ (MPa)	C (kg/m^{2}min$^{1/2}$)	λ (W/mK)
(Kheradmand, et al. 2018) [**15**]	Geopolymeric cement mortars	10%, 20% and 30% addition by wt. of solid constituents	13-16 (Ref) 2.5-10 (PCM)	1.0-2.3 (Ref.) 1.0-2.0 (PCM)	0.4-1.0 (Ref.) 0.15-0.40 (PCM)	…
(Shadnia, et al. 2015) [**16**]	Geopolymeric cement mortars	5%, 10% and 15% substitution of sand by vol.	25-26 (Ref.)[a] 15-21 (PCM)[a]	…	…	…
(Aguayo, et al. 2016) [**17**]	Cement mortars with quartz sand	Two PCMs (M and E) used as sand replacement at vol. fractions 5%-20%	45 (Ref.) 27-40 (PCM-M) 46-60 (PCM-E)	5.5 (Ref.) 3.0-4.7 (PCM-E) 6.0-6.5 (PCM-M)	…	…
(Šavija, et al. 2017b) [**18**]	Engineered cementitious composite containing blast furnace slag, limestone filler and PVA fibers	10%, 20% and 50% substitution of limestone filler by vol.	49 (Ref.) 35-43 (PCM)	12 (Ref.) 9-11.5 (PCM)	…	…
(Haurie, et al. 2016) [**19**]	Single-layer cement mortars containing glass fibers, organic additives, mineral pigments and	10% and 20% addition by wt. of mortar mixture	4.2 (Ref.) 2.36-4.12 (PCM)	…	…	0.51-0.54 (Ref.) 0.42-0.49 (PCM)

	resins					
(Cunha, et al. 2018) [**20**]	Cement mortars containing varying amounts of fly ash and polyamide fibers	22% addition by wt. of solid constituents	12-30 (Ref.) 5-12.5 (PCM)	3.5-7 (Ref.) 1.5-4.3 (PCM)	0.14-0.38 (Ref.) 0.08-0.25 (PCM)	…
(Cunha, et al. 2015a) [**21**]	Cement mortars with 32.5N and 42.5R cement binders	20%, 40% and 60% substitution of sand by wt.	32.5N cement 30 (Ref.) 12-20 (PCM) 42.5R cement 12 (Ref.) 4-7 (PCM)	32.5N cement 7.3 (Ref.) 4-7 (PCM) 42.5R cement 5 (Ref.) 1.8-3.0 (PCM)	…	…
(Jayalath, et al. 2016) [**22**]	Cement mortar	3% to 55% substitution of aggregates by vol.	43 (Ref.) 22-38 (PCM)	…	…	1.5-1.7 (Ref.) [a] 1.0-1.5 (PCM) [a]
(Lecompte, et al. 2015) [**23**]	Cement mortars containing limestone filler	14.8%, 22.1% and 29.3% addition by vol. of solid constituents	60.5 (Ref.) 16.3-30.0 (PCM)	5.3 (Ref.) 2.4-3.4 (PCM)	…	0.70-0.80 (Ref.)[a] 0.54-0.65 (PCM)[a]
(Joulin, et al. 2014) [**24**]	Cement: sand (1:2.7 w/w) mortar	19.4% addition by wt. of solid constituents	…	…	…	0.65 (Ref.) 0.37 (PCM)
(Ricklefs, et al. 2017) [**25**]	Cement mortars with quartz sand	10% and 20% addition by vol. of the mortar	…	…	…	1.50-1.77 (Ref.) 1.27-1.46 (PCM)
(Guardia, et al. 2019) [**26**]	Cement-lime mortars with and without perlite and cellulose fibers	10% and 20% addition by vol. of the mortar	9.4-14.3 (Ref.) 4.6-7.3 (PCM)	2.6-3.5 (Ref.) 1.7-2.4 (PCM)	0.35-1.08 (Ref.) 0.28-0.53 (PCM)	0.16-0.29 (Ref.) 0.19-0.32 (PCM)

f_c = Compressive strength at 28 days
$f_{t,b}$ = Flexural strength at 28 days
C = Capillary absorption coefficient
λ = Thermal conductivity
[a] depending on the assessment method used

This study examines the use of microencapsulated PCMs in the development of a TRM system for combined thermal and structural upgrading. The addition of a commercial microencapsulated PCM to a commercially available ready mixed polymer modified cement mortar is considered, aiming to increase the thermal mass of the latter to a degree that this could function as an overlay for passive building applications. The main evaluation criterion adopted is the attenuation and shifting of thermal peaks, without compromising the mechanical performance of the composite. The proposed system may be applied when the renovation scheme focuses on improving the thermal mass of the building envelope, or when restrictions regarding the use of other insulation methods exist (e.g. space constraints precluding bulky installations or limitations concerning the use of conventional thermal insulation layers that can alter the architectural character of listed buildings).

2 Materials and methods

2.1 Materials

2.1.1 Reference mortar mixture

In this study, a commercially available ready mixed polymer modified cement mortar, produced by Tsircon® Co Ltd, was used as reference material. This product is classified as R4 structural repair mortar, according to EN 1504-3 [**27**]. In addition to cement, fine aggregates (sand) and polymeric admixtures, this mortar also contains a viscosity modifying agent and short polypropylene fibers.

2.1.2 Microencapsulated PCM

A microencapsulated paraffin PCM (Nextek 37D), commercialized by Microtek Laboratories® Inc, was added to the polymer modified mortar in various quantities. This PCM is in the form of white dry powder and has a mean particle size in the range of 15-30 μm. Figure 1 shows the spherical morphology of the aforementioned PCM and also reveals a variation of its particle sizes. According to the product's specifications, the melting point is around 37 ^{o}C and the heat of fusion is ≥ 190 J/g. Differential Scanning Calorimetry data provided by the manufacturer show that the onset of the phase changing stage occurs at about 33 ^{o}C. The heat flux versus temperature curves exhibit peaks at 36-37 ^{o}C and give

normalized enthalpy values 210-214 J/g, thus verifying the declared melting temperature and heat of fusion. Furthermore, according to the manufacturer, this microencapsulated PCM exhibits very high temperature stability and shows less than 1% leakage when heated to 250 ^{o}C. Static contact angle measurements performed by the authors using the sessile drop technique indicated the hydrophobic nature of the microencapsulated PCM used (contact angles > 95^{o}).

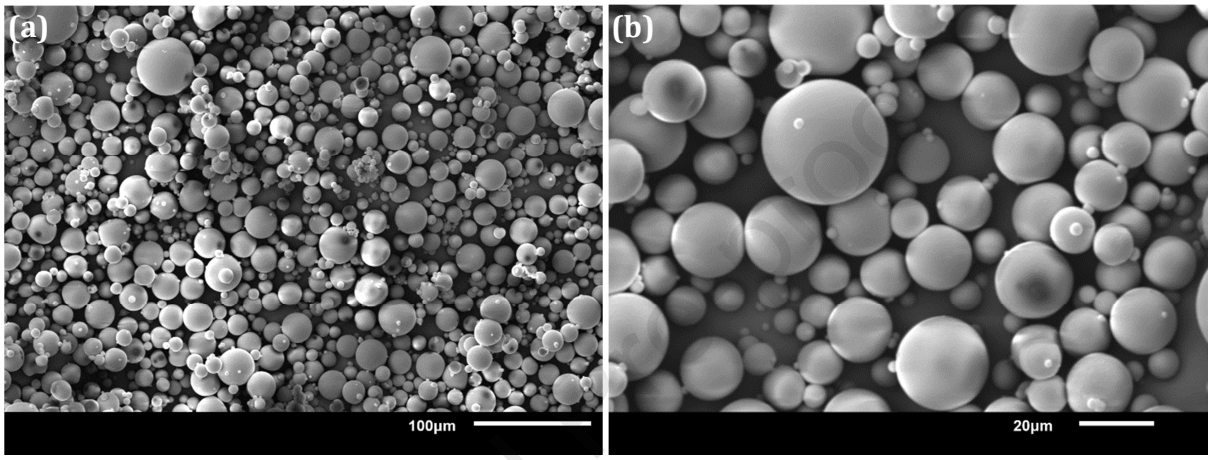

Figure 1. (a) Low and (b) high magnification SEM images showing the morphological characteristics of the microencapsulated PCM powder used.

2.2 Mix design, production and sampling

Mix designs with 5%, 10% and 20% PCM addition, by weight of the powder components of the ready mixed reference mortar, were produced in the laboratory. Before wet mixing, the PCM microcapsules were dry mixed with the powder mortar.

Preparation, curing and conditioning of the test specimens were carried out in accordance with EN 12190 [**28**] for polymer hydraulic cement mortars. All the mixtures were prepared using a standard 24 ltr capacity mortar mixer set at low speed (103 rpm). Initially, the amount of water suggested by the mortar supplier for reaching workable consistency (0.125 ltr per kg of mortar powder) was added to the bowl of the mixer. The solid constituents (i.e. the blend of the powder mortar mix components and the PCM microcapsules) were then added and the mixture was mixed for at least 2 min. After this period, the consistency of the fresh mixture was assessed using the EN 1015-3 [**29**] flow

table test method. A target consistency of 165 ± 5 mm was set. In case this was not achieved with the initial quantity of water used, additional water was gradually introduced to the mixture and the materials were kneaded until the desired consistency could be attained. The final quantities of water used in each mortar composition and the respective flow values obtained are reported in Table 2. Higher water demand with increasing PCM dosage was noted, in line with the findings of Coppola, et al. [**30**], Kheradmand, et al. [**15**] and Sanfelix, et al. [**14**]. According to the aforementioned researchers, water demand can increase substantially due to the higher specific surface area of the PCM microparticles.

Table 2. Quantities of water used in the mortar compositions prepared, expressed as ratios with respect to the solid constituents' weights, and corresponding consistencies assessed from flow table tests.

Mortar composition	Water to solids ratio (ltr/kg)	Consistency at fresh state (mm)
0% PCM	0.126	160
5% PCM	0.229	166
10% PCM	0.234	167
20% PCM	0.244	168

Prisms measuring 40 × 40 × 160 mm, cast in standard metallic molds, and plates measuring 30 × 150 × 170 mm, cast in customized molds made of shuttering plywood, were prepared with the fresh mixture. In both cases, the molds were filled in two equal layers and each layer was compacted with 60 jolts of a jolting apparatus. Immediately after casting, the molds were covered with polyethylene film. After 24 h, the specimens were demolded and wrapped in polyethylene bags for 48 h. They were then unwrapped and stored for 25 days in controlled laboratory conditions (24 ± 2 ^{o}C and 45 ± 5% RH).

2.3 Testing methodologies

2.3.1 Scanning electron microscopy

The reference and PCM-enhanced composites were characterized using a JEOL, JSM-6610 LV scanning electron microscope (SEM), equipped with a BRUKER type QUANTAX

200 energy dispersive X-ray spectrometer (EDS). The effect of microencapsulated PCM addition on the microstructural characteristics of the mortars was investigated using secondary electron images (SEI) from representative samples, mounted on double-sided carbon tape and sputter-coated with Au.

2.3.2 Assessment of physical properties

The apparent (bulk) density and open porosity of the materials were assessed via vacuum assisted saturation [**31**]. Oven dried mortar prisms (40 × 40 × 160 mm) were placed into an evacuation vessel (Figure 2a) under vacuum for a period of 2 h in order to eliminate the air in their pores. Afterwards, water was slowly introduced into the vessel until complete immersion of the specimens. The vessel was returned to atmospheric pressure and the specimens were left submerged for 24 h to achieve saturation. Each specimen was then weighted submerged in water (m_h), while the mass of the water-saturated specimens (m_s) was also measured. The apparent density (ρ_b) was expressed as the ratio of the mass of the dry specimen to its apparent volume:

$$\rho_b = \frac{m_d}{m_s - m_h}\rho_{rh} \quad (1)$$

where ρ_{rh} is the density of water.

The open porosity (p_o) was determined from the ratio between the volume of open pores and the apparent volume of the specimen:

$$p_o = \frac{m_s - m_d}{m_s - m_h}100 \quad (2)$$

MIP measurements were also performed on fragments acquired from the specimens used for the physico-mechanical tests, aiming to examine changes in the average pore diameter and pore size distribution of the studied composites. A Micromeritics (AutoPore IV 9520) mercury intrusion porosimeter was used for these measurements; this has a low-pressure upper limit of 50 psia, while in the range of high values it generates pressures up to 60,000 psia.

The water absorption coefficient (C) due to capillary action was assessed as per EN 1015-18 [**32**]. From each composition, six half-prisms (40 × 40 × ~80 mm) obtained after the flexural failure of specimens previously subjected to three-point bending were tested. The long faces of the test units used in the water absorption tests were sealed with epoxy resin. Following oven dying at 65 ^{o}C, the specimens were placed in plastic trays, with the broken faces immersed in deionized water up to a depth of 5 mm (Figure 2b). The specimens' weight was measured as a function of the time lapsed and the absorption coefficient was calculated from the recordings made at 10 (m_1) and 90 (m_2) minutes:

$$C = 0.1(m_2 - m_1) \tag{3}$$

In equation (3) m_1 and m_2 are measured in grams and the units of C are kg/m^{2}min$^{1/2}$.

(a) (b)

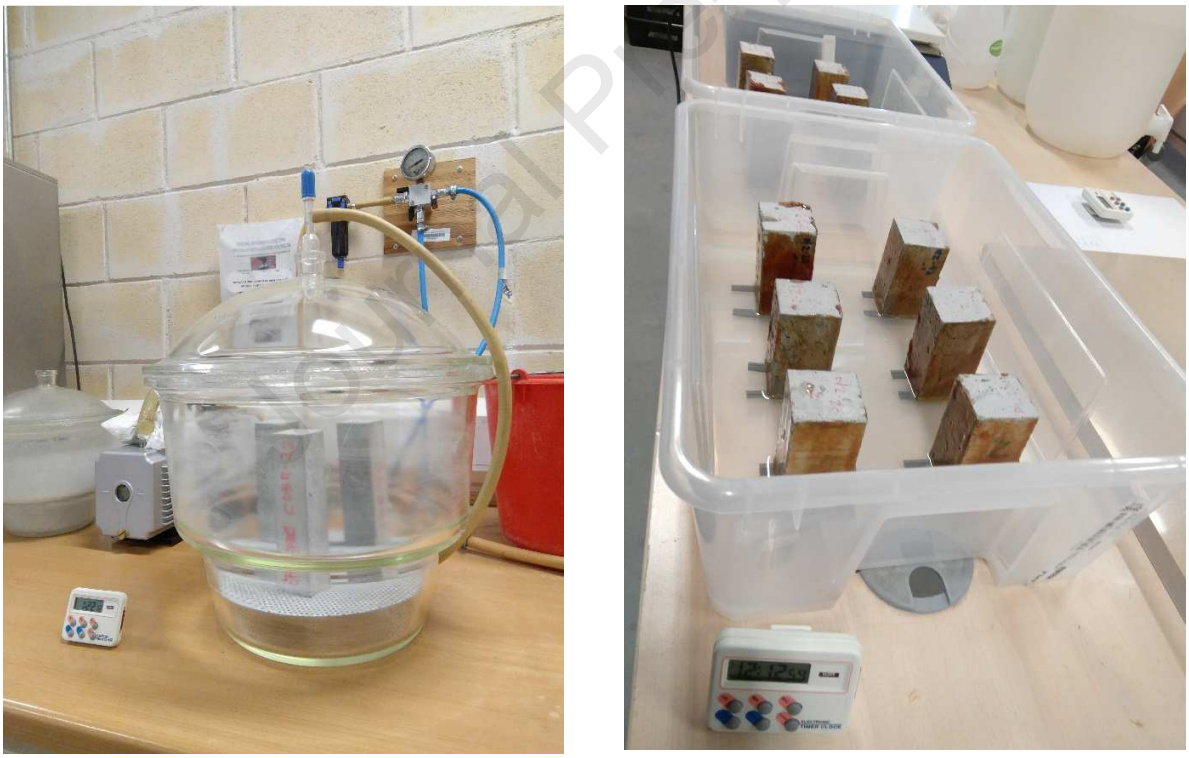

Figure 2. Test set-ups for the determination of the physical properties of mortars: (a) Vacuum assisted saturation for the evaluation of apparent (bulk) density and open porosity; (b) Water absorption experiments for the determination of the capillary absorption coefficient.

2.3.3 Assessment of mechanical properties

Tests for the determination of the mortars' mechanical properties were carried out at 28 days from casting. The flexural and compressive strengths were assessed in accordance with EN 1015-11 [**33**]. The mean flexural strength of each mortar mix design was determined by subjecting six prisms measuring 40 × 40 × 160 mm to three-point bending. The prisms were placed into a flexural jig assembly with a ball-seated upper bearer and two roller supports spaced 100 mm apart (Figure 3a). The loading jig was fitted between the platens of a universal testing machine, onto which a 10 kN loading head was mounted. Loading was applied at a displacement-controlled rate of 0.005 mm/s, which resulted to specimen failure at times between 30 and 90 s.

After the three-point bending test and the failure of the prism specimens, the compressive strength of each mortar mix design was determined by load testing six of the resulting half prisms. Specimens were tested using a compression jig equipped with a spherically seated upper platen (Figure 3b). The jig was accommodated into a 300 kN capacity universal testing machine. Compressive stresses were again exerted under displacement control, by setting the speed of the machine's travelling head to 0.02 mm/s.

The mortars' modulus of elasticity was assessed as per EN 13412 [**34**], by subjecting prims measuring 40 × 40 × 160 mm to controlled axial compressive loading and monitoring the longitudinal strain generated as a function of the imposed stress. Three prims were tested from each mix design. The tests were again carried out on a universal testing machine with a 300 kN load-cell. A spherically seated upper false platen was placed between the machine's fixed loading plates, in order enable adequate alignment with non-parallel bearing surfaces. The deformation measuring instruments used in each test consisted of two 60 mm long strain gauges, attached on opposite faces of the test units, originally in contact with the casting mold. The test setup is shown in Figure 3c.

(a)

(b)

(c)

Figure 3. Test set-ups used for the implementation of loading tests: (a) Three-point bending of mortar prims and (b) compression testing of half-prims as per EN 1015-11 [**33**]; (c) Uniaxial compressive loading tests with deformation monitoring on mortar prisms fitted with strain gauges as per EN 13412 [**34**].

To examine the response of the materials at the elastic range, the specimens were initially subjected to three loading-unloading cycles, during which the exerted stress varied between 0.5 MPa and one-third of the expected failure stress. After the completion of the three cycles, the specimens were loaded up to failure. Throughout the testing procedure, loading was applied under deformation control, at a constant rate of 0.2 mm/min. The modulus of elasticity was estimated from the stress-strain data recorded during the three loading-unloading cycles, using linear regression. The experimental results yielded also enabled examining the stress-strain response of the materials up to a post-peak point corresponding to ca. 10% loss of load-bearing capacity. Therefore, measurements of strain at peak compressive stress could be obtained.

2.3.4 Assessment of thermal properties

Thermal conductivity (λ), thermal diffusivity (a) and specific heat capacity (c_s) were assessed, based on the analysis of the temperature response of the mortars to heat flow impulses. This was done using an ISOMET 2104 measuring instrument. The apparatus is equipped with a surface probe that is placed in direct heat contact with the test specimen. During the test, heat flow is excited by electrical heating of a resistor heater incorporated into the probe. Heat propagation into the tested medium is monitored via periodically sampled records of temperature over time. In this study, a probe with a thermal conductivity (λ) measuring range 0.30-2.0 W/mK at temperature gradients -15 ^{o}C to +50 ^{o}C was used. From every mix design, a single plate specimen (thickness × length × width = 30 × 150 × 170 mm) was examined. Measurements were carried out on three different positions across the surface of this specimen. Prior to testing, the specimens were placed inside an environmental chamber, at a controlled temperature of 25 ^{o}C, until thermal equilibrium was attained (minimum conditioning time 48 h). In order to verify that thermal equilibrium was achieved, the temperature of the specimens was constantly monitored with thermocouples attached to their upper and lower surfaces. The selected temperature conditions aimed to ensure that the PCM would remain at a steady (solid) state throughout the thermal tests.

The thermal properties of each specimen were automatically computed by the measuring instrument, following processing of the recorded data. At the range of

properties measured, the system has 5% accuracy and 3% reproducibility with respect to the readings made. It is noted that the system reports the volume, rather than the specific heat capacity of the tested materials. The specific heat capacity (c_p) was thus estimated from the volume heat capacity (c_v) and the volume (V_s) and dry mass (m_d) of each specimen as $c_p = c_v V_s / m_d$. The thermal diffusivity was evaluated by the testing system by dividing the thermal conductivity with the volume heat capacity measurement ($a = \lambda / c_v$). It is worth noting that, although the transient heat method hereby adopted differs from the standardized guarded hot plate method, it has been used in several research studies examining PCM-modified mortars (e.g. [**19**], [**35**], [**36**], [**37**]). This method is also prescribed in certain standards referring to soft rocks and soils [**38**].

For investigating the thermal performance of the mortars prepared under temperature variations, a customized test setup (Figure 4) was designed, based on relevant work by Shadnia, et al. [**16**], Young, et al. [**39**] and Ramakrishnana, et al. [**40**]. Tests were performed on mortar plates (the same as those tested with the transient heat method), attached on thermally insulated cubic test cells (side length = 450 mm). Five of the cells' walls were made of 70 mm thick extruded polystyrene (λ = 0.035 W/mK), while the mortar plates were attached on the remaining free face. The joints between the extruded polystyrene panels and along the perimeter of the mortar plates were filled with insulating foam and sealed with heat resistant silicone. The exterior surface of the extruded polystyrene walls was entirely covered with high-heat ducting insulation tape.

(a)

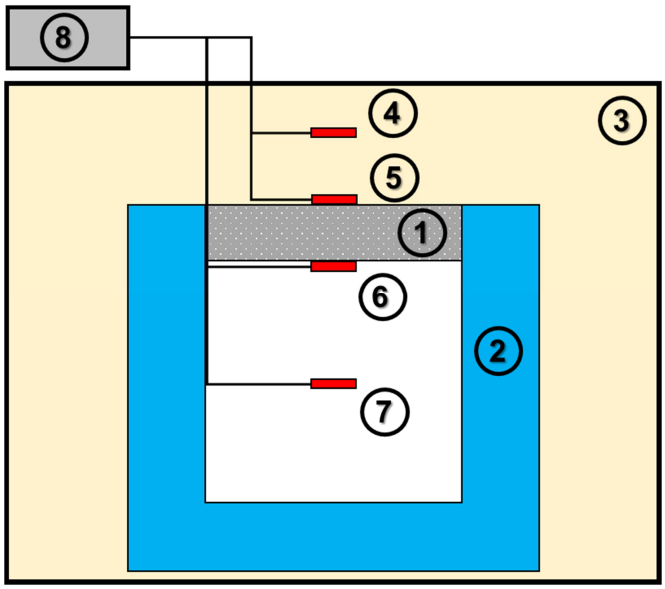

1. Mortar plate sample 3 x 15 x 17 cm
2. Extruded polystyrene thermal insulating enclosure 7 cm thick
3. Environmental chamber with controlled temperature variation
4. Thermocouple for measuring the ambient temperature inside the chamber
5. Thermocouple attached to the exterior surface of the sample
6. Thermocouple attached to the interior surface of the sample
7. Thermocouple for measuring the temperature inside the test cell
8. Data acquisition system

(b)

Figure 4. Schematic representation (a) and photograph (b) of the test set-up implemented to investigate the response of mortar plate samples to temperature variations in laboratory-controlled environment.

The test cells were placed inside a climatic chamber, where they were subjected to controlled sinusoidal variations of the ambient temperature. The experimental procedure aimed to produce a condition of unidirectional heat flow, in which the heat flux governing the temperature at the interior of the test cell develops through the thickness of the mortar plate, rather than through the insulated walls that possess higher thermal resistance. Indeed, the exterior surface of the mortar plate was exposed to convection within the chamber. Heat flow in the lateral direction was considered to be practically negligible, as all sides along the plate's perimeter were heavily insulated.

Sinusoidal variation of the ambient temperature as a function of time ($T_{sa}(t)$) was imposed over a cyclic period of P = 24 h:

$$T_{sa}(t) = \frac{T_{max} - T_{min}}{2} \sin\left(\frac{2\pi}{P} - \frac{\pi}{2}\right) + \frac{T_{max} - T_{min}}{2} + T_{min} \quad (4)$$

In the above equation T_{max} and T_{min} are the maximum and minimum values of the ambient temperature. These values were hereby taken as T_{max} = 45.6 ^{o}C and T_{min} = 8.8 ^{o}C, based on local climatic data for Cyprus. More specifically, the recordings of the Athalassa meteorological station from year 2010 to year 2018 for the spring-summer seasons (May-September) were considered. Emphasis was placed on the spring and summer months, because the response of building materials to the hot arid conditions that occur in Cyprus during this time of the year is critical. In each test, the temperature of the chamber was initially set constant to 20 ^{o}C for 24 h, in order to achieve thermal equilibrium. Subsequently, three sinusoidal cycles were implemented.

Four type-T thermocouple sensors were used for monitoring the temperature at different positions of the test setup. One thermocouple measured the ambient temperature of the chamber. Two thermocouples were centrally attached to the mortar plates to measure the temperature on the exterior and interior surface of the material. The fourth thermocouple was placed inside the test cell to record the temperature of the air at the mid-height of the cubicle enclosure. The thermocouples were connected to data acquisition systems that made recordings at regular intervals of 5 minutes.

3 Experimental results and discussion

3.1 Scanning electron microscopy (SEM)

SEM observations show that the porosity of the studied mortars significantly increases with increasing levels of microencapsulated PCM (Figure 5). This is consistent with other published works that have reported a less dense microstructure in PCM-enhanced mixtures (e.g. [**14**], [**20**], [**37**], [**41**]). The latter is primarily attributed to the high specific surface area of the PCM particles (see Figure 1), which notably increased the water demand of the mixtures hereby studied (see Table 2) ([**14**], [**15**], [**30**]).

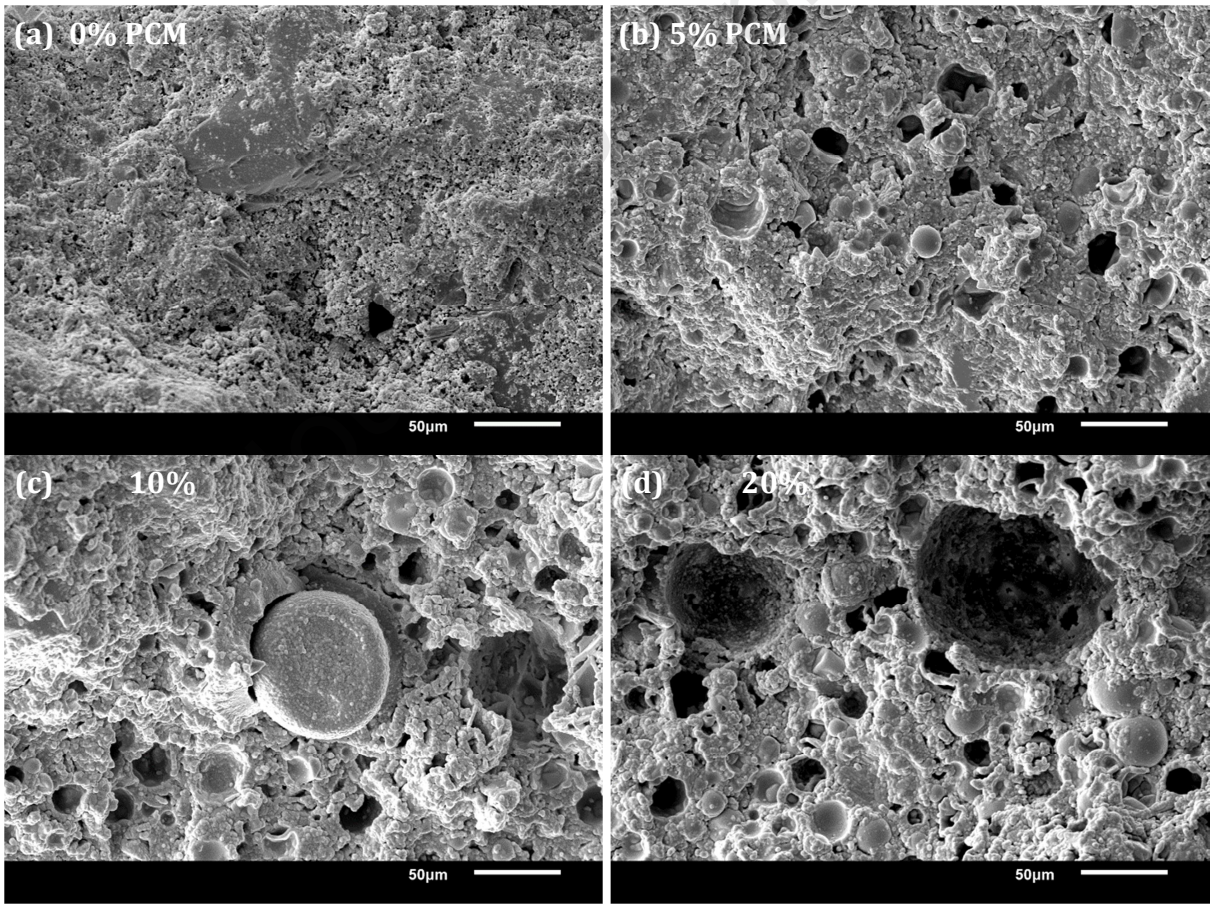

Figure 5. SEM images showing a gradual increase in porosity with increasing microencapsulated PCM dosage; mortar specimens containing (a) 0%, (b) 5%, (c) 10% and (d) 20% PCM.

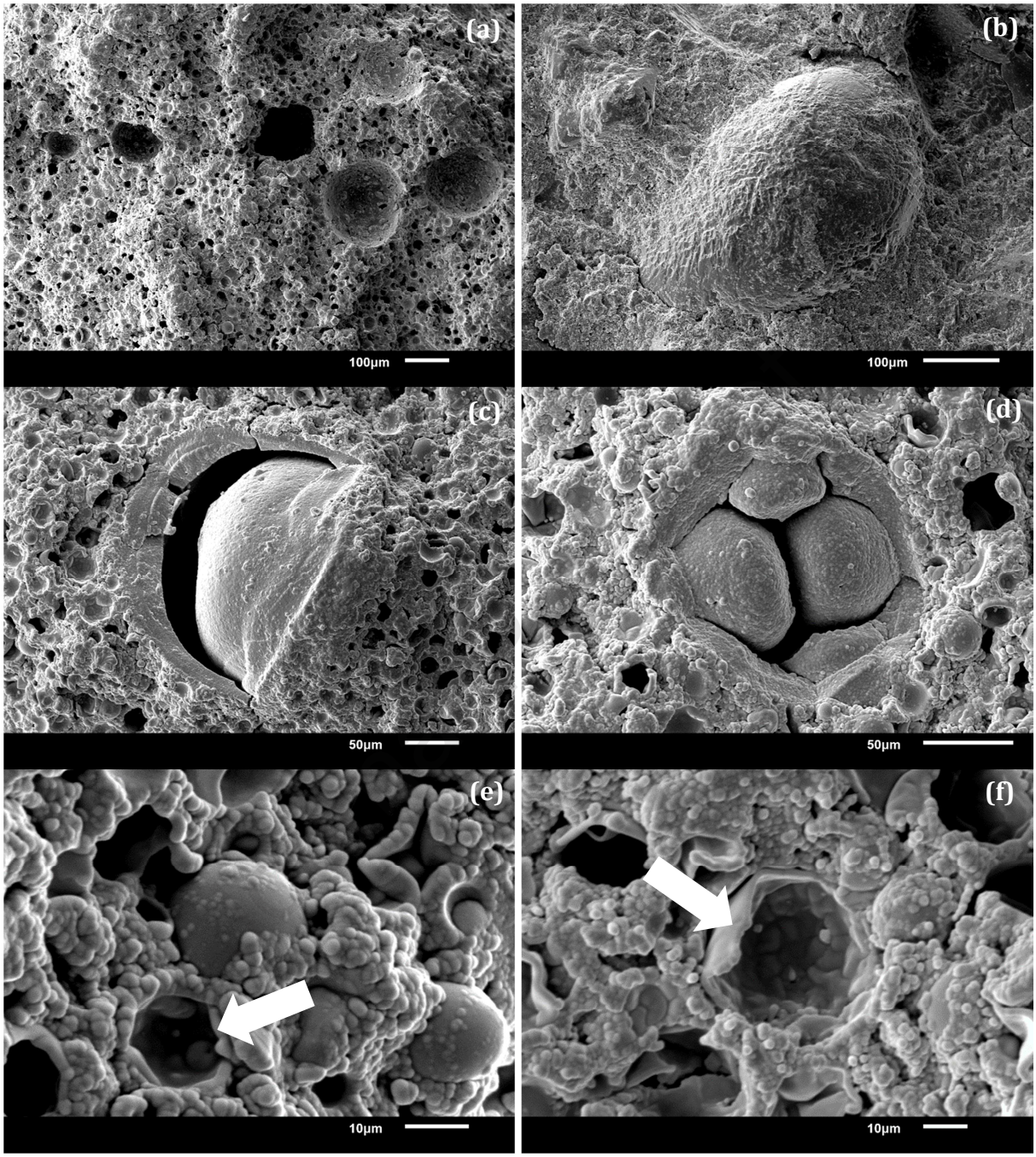

Figure 6. SEM images showing a number of microstructural features in the studied mortars; (a) Micro- and macro-pores in the mortar containing 20% PCM; (b) Strong and (c) Weak adhesion between the polymer modified cement paste matrix and the aggregate particles in the composites with 0% and 20% PCM, respectively; (d) Agglomerated PCM particles in the composite with 20% PCM; Broken PCM microcapsules (see arrows) in the mortars containing (e) 10% and (f) 20% PCM.

Figure 6a shows the abundance of micro-pores in the mortar containing 20% microencapsulated PCM, while a number of macro-pores can also be observed in the same Figure. The formation of the latter is closely related to the considerably weaker adhesion between the polymer modified cement paste matrix and the aggregate particles in the presence of microencapsulated PCM (compare Figure 6b with 6c). This effect probably becomes more prominent in the presence of damaged microcapsules, since the leaked paraffin may significantly weaken the bond between the aggregates and the cementitious matrix [**42**].

Agglomerated PCM particles were also detected in the PCM-enhanced mortars. Their presence was more pronounced in the composite containing 20% PCM (Figure 6d). This phenomenon is presumably attributed to the breakage of a number of PCM microcapsules (Figure 6e and 6f) during the mixing process, and subsequently to the leakage of paraffin throughout the matrix. Non-encapsulated paraffin may act as an adhesive, thus promoting the agglomeration of microcapsules, particularly in mixtures with relatively high PCM additions. Such agglomerates tend to reduce the homogeneity of the mixture, thereby negatively affecting the performance of the hardened composites. In fact, the leaked paraffin and the resulting agglomerates can increase the viscosity of the mixture, thus facilitating the entrapment of air and the formation of macro-voids ([**41**], [**43**]). This process could comprise another potential explanation for the enhanced macro-porosity observed, mainly in the mortar with 20% PCM addition (Figure 6a).

3.2 Physical properties

The experimentally assessed physical properties of the mixtures hereby examined are given in Table 3. Figure 7 plots the ratios of the densities, porosities and capillary absorption coefficients with respect to the properties of the reference composition, as a function of microencapsulated PCM addition.

Table 3. Average physical properties (Coefficient of Variation) determined from vacuum saturation and water absorption tests on polymer modified cement mortar samples containing 0% (reference composition), 5%, 10% and 20% PCM.

Property	No. of tests	Mortar composition			
		0% PCM	5% PCM	10% PCM	20% PCM
Apparent (bulk) density - ρ_a (kg/m^3)	3	2080 (0.0%)	1823 (0.3%)	1593 (0.0%)	1423 (0.4%)
Open porosity - p_o (%)	3	9.28 (1%)	9.93 (3%)	12.66 (1%)	15.70 (3%)
Absorption coefficient - C (kg/m^{2}min$^{1/2}$)	6	0.03 (8%)	0.03 (5%)	0.03 (15%)	0.04 (15%)

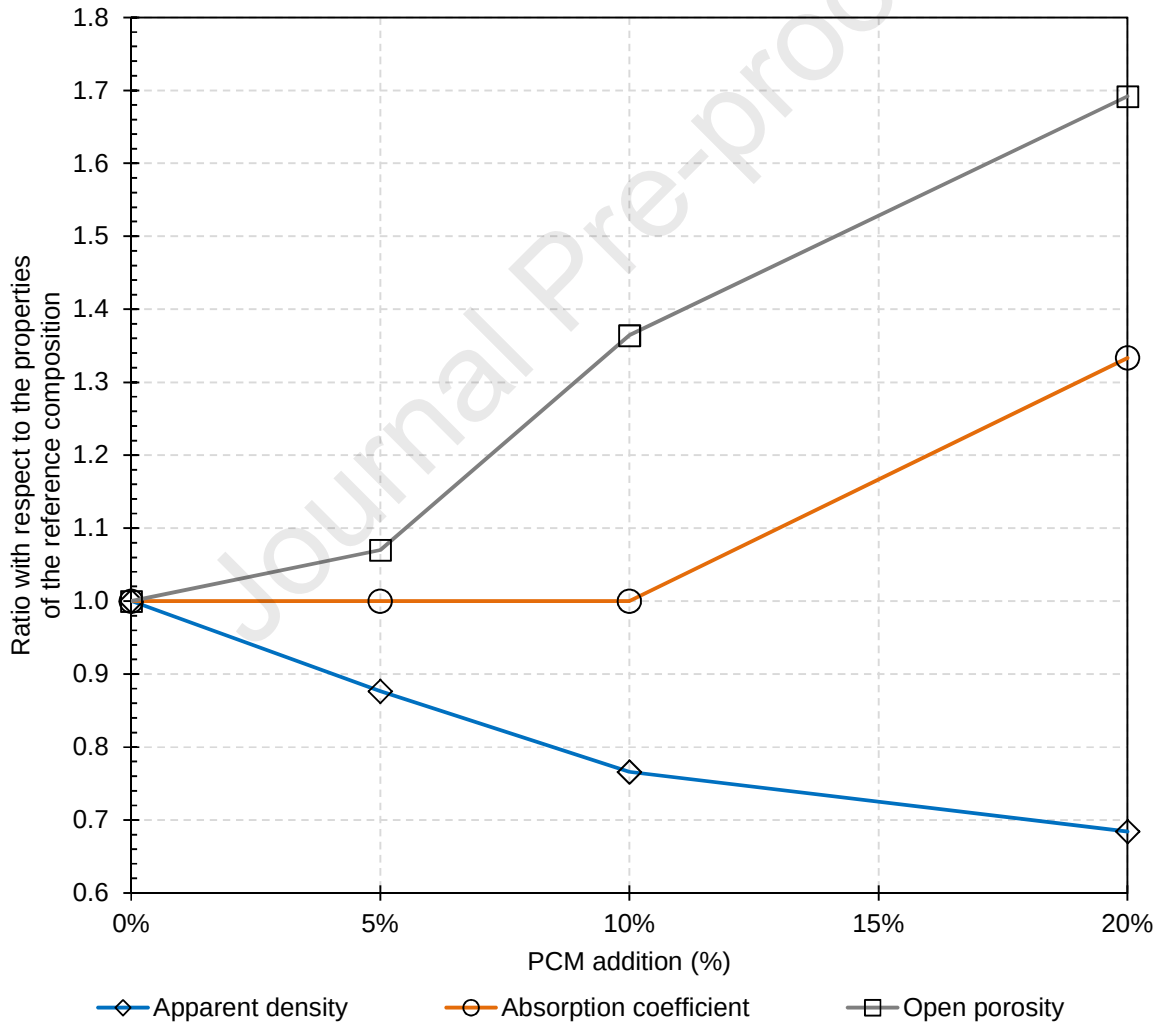

Figure 7. Ratios of average apparent (bulk) density, open porosity and capillary absorption coefficient with respect to the properties of the reference composition (0% microencapsulated PCM), plotted as a function of microencapsulated PCM percentage addition.

An increase in the total volume of open pores and a reduction in the apparent (bulk) density of the samples is observed with increasing amounts of microencapsulated PCM. The accessible porosity of the reference mortar is 9.3%. For 5%, 10% and 20% microencapsulated PCM addition, this value increases by 10%-69%, rising to 9.9%, 12.7% and 15.7%, respectively. These results are in agreement with the SEM observations, which showed a gradual increase in porosity with increasing microencapsulated PCM dosage (see Figure 5). Furthermore, the results acquired here are in line with the outcomes of X-ray tomography and MIP tests performed by Djamai, et al. [**41**]. The aforementioned researchers pointed out that, increasing the microencapsulated PCM dosage in cementitious mortars, generally leads to higher volume of accessible pores. The use of microencapsulated PCMs may also lead to the formation of macro-pores with diameters an order of magnitude larger than those present in mixtures without microencapsulated PCM. This scenario is strongly supported by the SEM observations hereby reported, which reveal that macro-porosity is more evident in the mixture with 20% PCM addition (see Figure 5d and Figure 6a). The significant increase in the porosity of the PCM-enhanced composites hereby studied is mainly attributed to the higher water demand required to reach the desired consistency at fresh state (see Table 2); the latter is due to the fineness of the microencapsulated PCM additive.

The recorded reduction in the density of the studied mortars is almost proportional to the percentage of microencapsulated PCM added to the mixtures. It ranges from 13% for 5% microencapsulated PCM addition to 33% for 20% microencapsulated PCM addition. Analogous results are reported in several other studies (e.g. [**15**], [**16**], [**19**], [**44**], [**45**], [**46**], [**47**]) for a variety of PCM-modified cementitious materials, including geopolymer mortar and concrete. The low unit weight of the PCM material hereby used (paraffins generally have densities < 1250 kg/m^3, according to the data reported in [**8**]) is considered to be the main parameter affecting the density of the hardened composites.

The MIP results provide significant information on the pore structure of the studied mortars. As can be seen in Figure 8, an increase of the average pore size with increasing levels of microencapsulated PCM addition is observed. Similar results have also been reported by Djamai, et al. [**41**], following the addition of different amounts of PCM (i.e. 5-

15% by wt.) in cementitious mortars. According to the aforementioned researchers, this increase in pore size is mainly attributed to the fact that cement grains coated with PCM particles cannot participate in the hydration process, due to the limited access of water to cement. As a result, the pore spaces of the PCM-enhanced composite are occupied by fewer hydration products, thus resulting in a microstructure with larger pore diameters, compared to specimens without PCMs. The presence of damaged PCM capsules further inhibits the hydration reactions in cement mortars, probably due to the leakage of paraffin and its interference with the surrounding material [**48**]. In the mortars hereby studied, this effect becomes more pronounced with increasing percentage of microencapsulated PCM addition. As shown in Figure 8, a nearly twofold increase of the average pore diameter is observed from 0% to 5%, as well as from 5% to 10% microencapsulated PCM addition, whilst a smaller increase is acquired by increasing the amount of PCM from 10% to 20%.

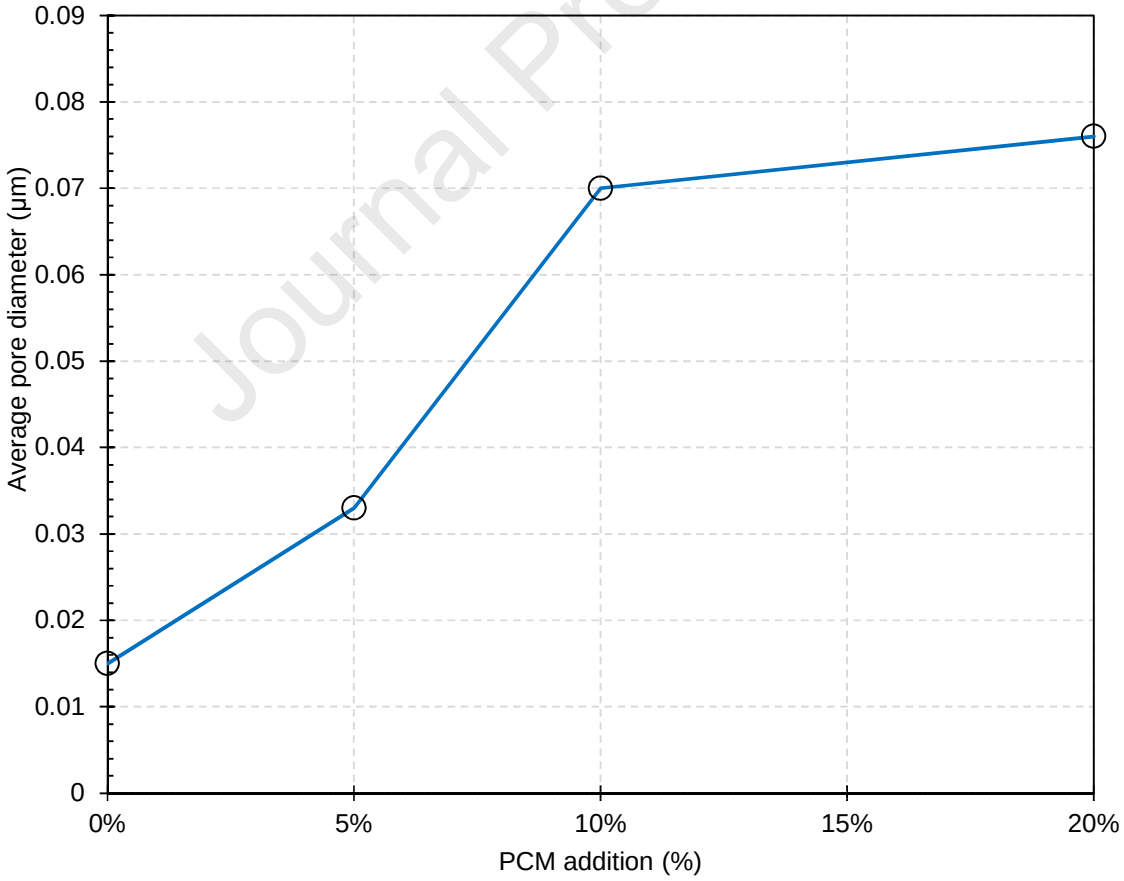

Figure 8. Average pore diameter values, estimated via mercury intrusion porosimetry (MIP), plotted as a function of microencapsulated PCM percentage addition.

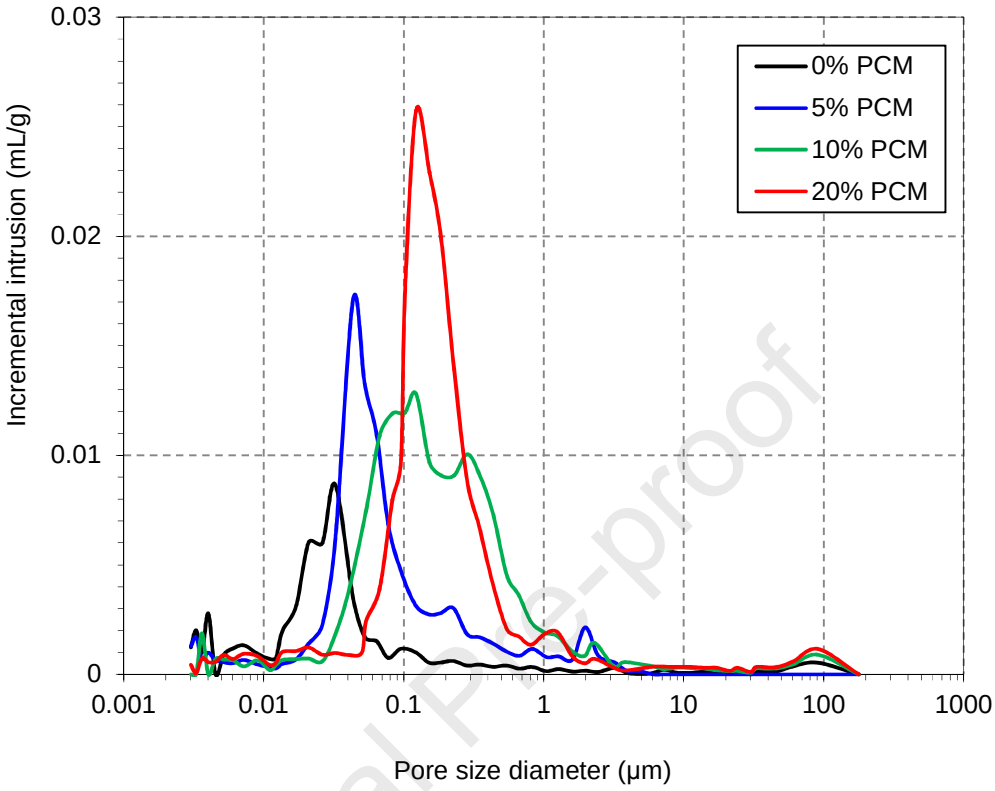

Figure 9. Pore size distributions determined by mercury intrusion porosimetry (MIP) on polymer modified cement mortar samples containing 0% (reference composition), 5%, 10% and 20% PCM.

Regarding the pore size distribution of the studied mortars, Figure 9 reveals a shift towards larger pore sizes in the PCM-enhanced mortars. This modification of the pore structure agrees well with the higher porosity and lower density values of the specimens containing PCMs (see Table 3). In the reference mortar hereby studied, a main peak exists between ca. 0.01 and 0.05 μm, and a smaller peak appears at ca. 0.1 μm. In the mortar containing 5% PCM, the same peaks have been shifted to higher values (ca. 0.02-0.15 μm and 0.25 μm for the main and secondary peak, respectively), while a new peak also appears at 2 μm. These results confirm that larger pores tend to become more abundant due to the addition of microencapsulated PCM. A further shift towards larger pore sizes is observed in the composite with 10% PCM. In fact, the latter shows two partially overlapping peaks within the ca. 0.03-2 μm pore size range, as well as a significantly smaller peak at even larger pore sizes (i.e. 2-3 μm). The mixture containing 20% microencapsulated PCM shows

a prominent increase in the volume of pores between ca. 0.05 and 0.6 μm, while two smaller peaks can also be detected at larger pore sizes (i.e. 0.8-2 μm and 2-3 μm). All the aforementioned changes in the pore structure are consistent with the microstructural features observed by SEM. They are also in line with the results of the vacuum saturation tests, which showed a gradual increase in porosity with increasing microencapsulated PCM content.

Comparing the capillary absorption coefficients of the microencapsulated PCM-enhanced mortars with those of the reference mix design, no differences are noted at dosages up to 10%. For 0% to 10% microencapsulated PCM addition, the experimental results are consistently around 0.03 kg/m^{2}min$^{1/2}$. A higher absorption coefficient was obtained for the mixture containing 20% microencapsulated PCM; 0.04 kg/m^{2}min$^{1/2}$. It is interesting to note that all compositions tested can be graded as W2 mortars (C < 0.20 kg/m^{2}min$^{1/2}$), which is the superior absorption class specified in EN 998-1 [**49**] for masonry renders and plasters. This implies that, despite the increase reported in capillarity at high microencapsulated PCM dosages, mortars aligning with standardized performance requirements may still be produced.

Characteristic curves showing average water absorption by capillarity as a function of the square root of time ($t^{1/2}$) for the four different mortar compositions examined are given in Figure 10. The measurements taken indicate that, at early time stages, capillary absorption varies linearly with $t^{1/2}$, as expected [**31**]. As the test proceeds, the cumulative water absorption per unit surface area falls below what would have been expected from the classical unsaturated flow theory. This is likely attributed to the reactivity of cement with water [**31**]. However, it may also be the result of the development of bimodal pore size distribution with microencapsulated PCM addition, as indicated by the MIP tests (Figure 9). Hall and Raymond Yau [**50**] and Ioannou et al. ([**51**], [**52**]) showed that bimodal cementitious materials can indeed exhibit anomalous water sorptivity of the type hereby observed. These researchers explained deviation from linearity during capillary absorption tests, by considering the retarding effect of gravity on the capillarity of coarse pores. Both the experimental results yielded in this study (see for example Figure 9) and the data reported in the literature, strongly support that microencapsulated PCM addition poses a

significant effect on the pore size distribution of cementitious composites, subsequently influencing their capillary absorption. The overall impact can be quite complex. Breakage and/or agglomeration of capsules (see Figure 6d-f), may result in the entrapment of air due to increased viscosity in the fresh state and, in turn, to the formation of macro-voids in the hardened composites ([**41**], [**53**]). At the same time, some filling effect may also take place [**54**]. It is thus possible that the pore structure and absorption behavior of the tested materials have indeed been influenced by more than one of the aforementioned mechanisms. However, a deeper insight into the anomaly observed would require further investigation and additional capillary absorption experiments with non-reactive liquids (e.g. organic solvents), which is beyond the scope of this paper.

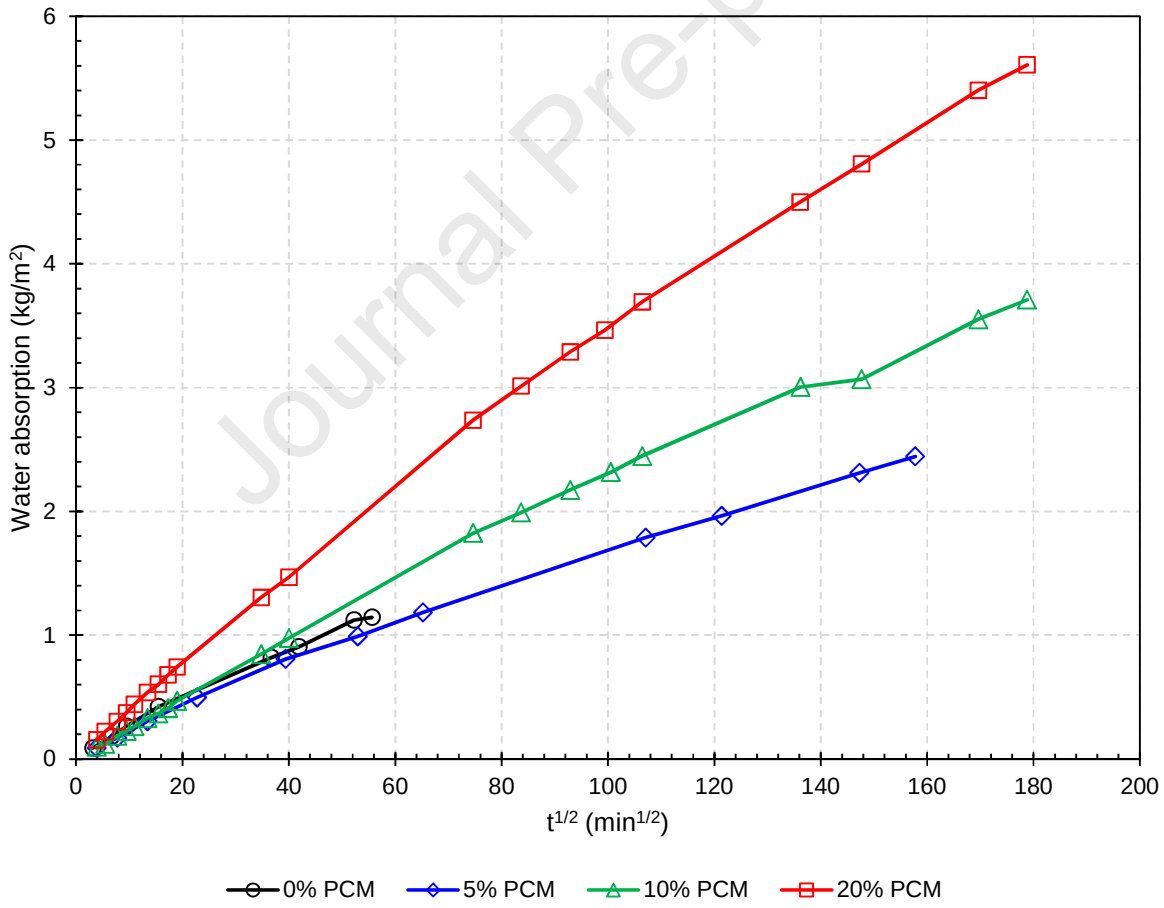

Figure 10. Characteristic curves for the evolution of water absorption by capillarity as a function of the square root of time for the four different mortar compositions hereby examined. The data points presented in each case correspond to the average water absorption measured at a given time point following the testing of six specimens. It is noted that individual measurements taken from different specimens originating from the same composition at any given time point have coefficients of variation from 3.5% to 17%.

Nevertheless, comparing the suction curves for the 5% and 10% microencapsulated PCM mortars (Figure 10), which yielded similar capillary absorption coefficients, it is shown that the initial rate of water absorption is not significantly affected by the microencapsulated PCM addition. However, the influence of microencapsulated PCM content on the suction curves of the two aforementioned mortars is evident when absorption stops following the $t^{1/2}$ law. At this stage, the rate at which the mortar containing 10% microencapsulated PCM absorbs water is clearly higher, compared to that of the mortar containing 5% microencapsulated PCM. It may thus be argued that the absorption coefficients, computed in accordance with EN 1015-18 [**32**], describe only the early stage absorption rates and are thus not entirely representative of the full capillary absorption behavior of PCM-enhanced mortars.

3.3 Mechanical properties

Table 4 presents the average compressive and flexural strengths derived, along with the elastic moduli and the axial strains at peak compressive stress, measured from static compression loading tests. Figure 11 plots the ratios between the mechanical properties of the microencapsulated PCM-modified mixtures and the reference mix design. The results show an almost exponential decrease in the load-bearing capacity and elastic modulus with increasing percentage of microencapsulated PCM addition. The reference mortar gave an average flexural strength of 8.6 MPa, while the microencapsulated PCM mortars have flexural strengths in the range 6.2 to 4.8 MPa. A more acute effect is noted in the results of compression tests. The lower amount of microencapsulated PCM addition considered (i.e. 5%) caused a nearly twofold reduction in compressive strength; from ca. 64 MPa to 37 MPa. For 10% and 20% microencapsulated PCM addition, the compressive strength dropped further to ca. 22 MPa and 14 MPa, respectively. The elastic modulus results follow the same trend noted for the compressive strength. The average elastic modulus of the reference mortar is 31.2 GPa. The respective values obtained after the addition of microencapsulated PCM were 52% to 86% lower. The test results agree with the findings of several other studies, which report analogous reduction in the mechanical properties of PCM-enhanced cementitious mortars (see Table 1).

Table 4. Average mechanical properties (Coefficient of Variation) determined from load tests on polymer modified cement mortar samples containing 0% (reference composition), 5%, 10% and 20% PCM.

Property	No. of tests	Mortar composition			
		0% PCM	5% PCM	10% PCM	20% PCM
Flexural strength - $f_{t,b}$ (MPa)	6	8.55 (9%)	6.19 (12%)	5.56 (4%)	4.82 (8%)
Compressive strength - f_c (MPa)	6	64.4 (5%)	37.0 (2%)	22.2 (5%)	14.4 (2%)
Elastic modulus - E_s (GPa)	3	31.2 (5%)	14.9 (4%)	7.95 (11%)	4.44 (3%)
Strain at peak comp. stress - ε_u (μm/m)	3	3300 (5%)	4300 (9%)	6200 (26%)	8700 (4%)

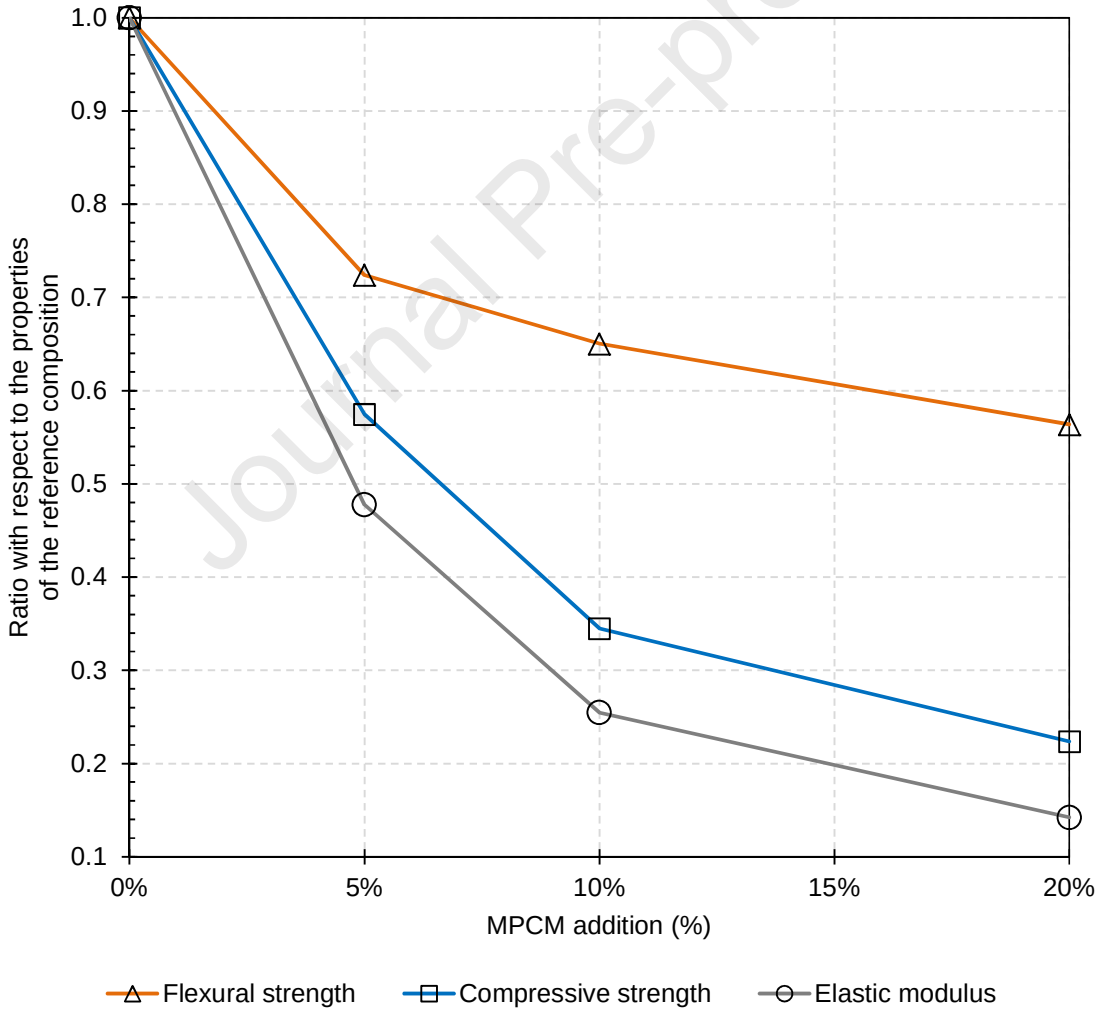

Figure 11. Ratios of average flexural strength, compressive strength and elastic modulus with respect to the properties of the reference composition (0% microencapsulated PCM), plotted as a function of microencapsulated PCM percentage addition.

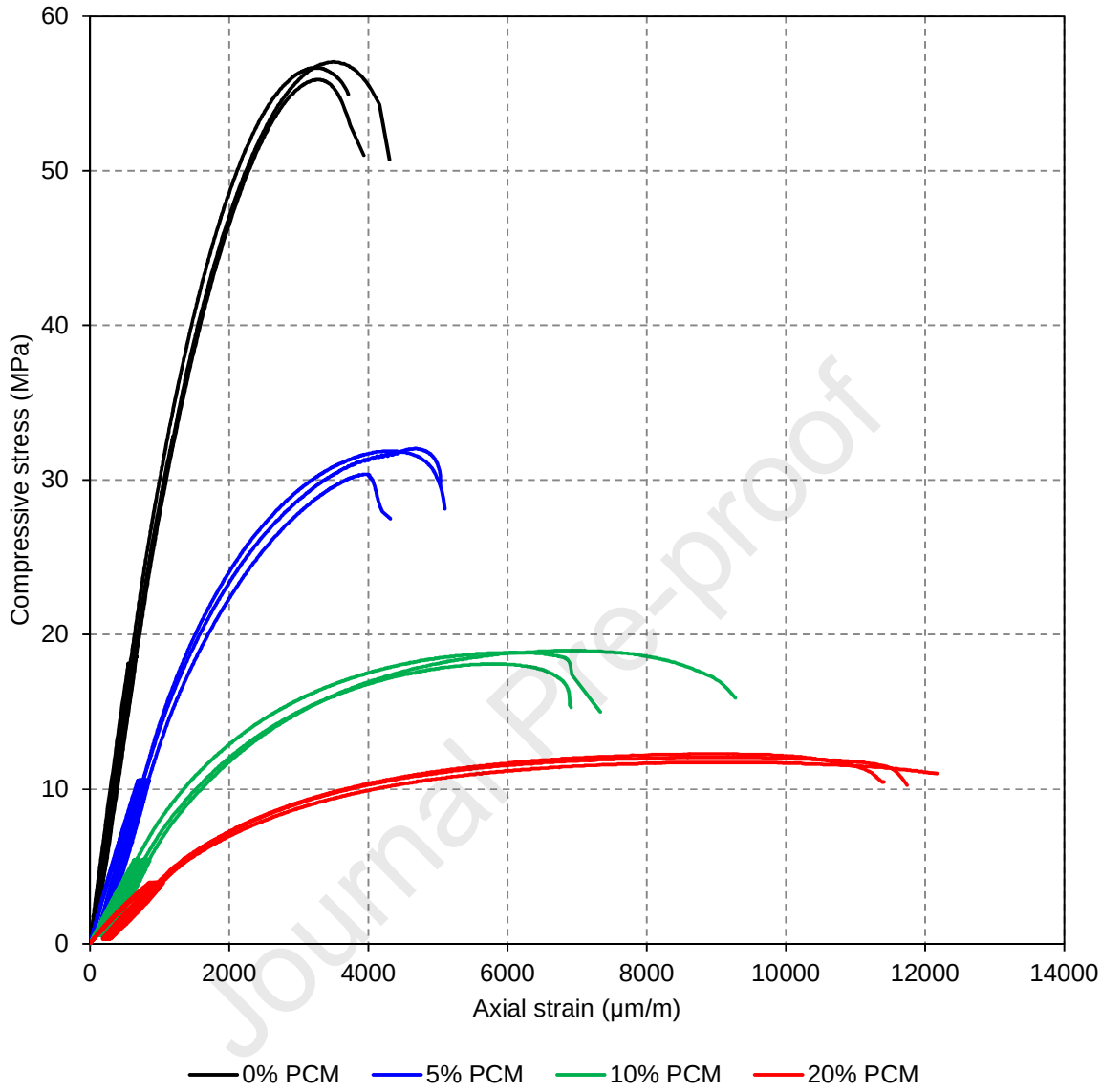

Figure 12. Stress-strain curves obtained by the implementation of uniaxial compressive loading tests as per EN 13412 [**34**] on mortar specimens containing 0%, 5%, 10% and 20% PCM. For each composition, the results obtained from 3 different test units are reported. Strain values correspond to the average reading of two strain gauges, attached on opposite faces of the test unit.

The stress-strain response of the tested samples is shown in Figure 12. The mortars exhibit a compressive behavior, which is typical of quasi brittle cementitious materials. An almost linear increase of axial deformations with increasing magnitudes of imposed stress is observed up to approximately 30% of the compressive strength. Beyond this limit, the stress-strain relationship becomes nonlinear. In the plastic regime, the response is

characterized by stress hardening up to the maximum allowable stress. This is followed by post-peak strain softening up to the ultimate strain sustained. In all cases, the descending softening branch is quite distinct, with a drastic loss of bearing capacity occurring after the exceedance of the material's strength. The experimental data indicate a significant influence of microencapsulated PCM addition on the hardening behavior of the composites. For the reference mortar, the peak compressive stress occurs at a strain ca. 3300 μm/m. This is similar to what is reported in the literature for conventional cementitious mortars of analogous strength [**55**]. The presence of microencapsulated PCM inclusions shifts the strain at which the peak compressive stress is attained to considerably higher levels. Subsequently, the ultimate failure strain also increases. The increase in the deformation capacity is more profound for 10% and 20% microencapsulated PCM addition; the average strains at peak compressive stress for these compositions were 6200 and 8700 μm/m.

The negative effect of microencapsulated PCM addition on the mechanical properties of the materials hereby examined can be primarily attributed to the lower strength and stiffness that the PCM capsules possess, in comparison to the polymer-modified cement paste matrix and the aggregate particles. Based on the micromechanical framework developed in Falzone, et al. [**56**], Fernandes, et al. [**57**] and Xu, et al. [**58**], the PCM microcapsules can be considered as soft inclusions surrounded by interfacial transition zones. Increasing the volume that the microcapsules occupy within the host matrix can result to higher elastic strains at low levels of uniaxial compressive loading (< 30% of the peak stress), as softer particles undergo larger deformations. This inevitably reduces the elastic modulus of the composite. Falzone, et al. [**56**] also comment that, at high microencapsulated PCM dosages (> 30% by vol.), the volume fraction of the interfacial transition zones grows substantially, and some tendency for microcracking-induced softening occurs. Such phenomena can further decrease the effective elastic modulus, since linear response is essentially lost at lower stress magnitudes. According to Wei, et al. [**59**] and Fernandes, et al. [**57**], the elastic mismatch between the host matrix and the microencapsulated PCM inclusions can promote crack blunting/deflection effects, as well as some stress relaxation at static strain rates. This can limit brittleness to some degree and

is possibly the reason for the enhanced deformation capacity that the microencapsulated PCM mortars exhibit.

As stated in Falzone, et al. [**56**], the maximum allowable stress in compression is linked to the percentage addition of the microencapsulated PCM because the capsules constitute the critical defect in the system. This notion is supported by the numerical study of Das, et al. [**60**]. The aforementioned researchers have shown that soft inclusions within cementitious composites subjected to external strains sustain lower stresses than the rest of the material constituents, due to their lesser stiffness. However, their response under loading is the one governing the failure of the composite. This is because their distinctively low bearing capacity is far inferior to that of the paste matrix and of the interfacial transition zones.

Nevertheless, it should be underlined that the strength achieved by the microencapsulated PCM-enhanced mortars hereby studied has not been solely dependent upon the weak nature of the capsules themselves. It was almost certainly influenced by the increased water demand (and subsequent rise of open porosity) caused by the microencapsulated PCM incorporation. In fact, the higher water-to-binder ratios in the PCM-enhanced mortars resulted in a less dense microstructure, as confirmed by SEM observations and the results of the physical property tests (see sections 4.1 and 4.2). The increased micro- and macro-porosity, the presence of agglomerated PCM particles, as well as the weak adhesion between the cementitious matrix and the aggregates in the composites containing PCMs, are considered among the main reasons for the reduction in the mechanical properties with increasing microencapsulated PCM content. Regarding the agglomerated PCM particles, in particular, it should be underlined that they can potentially act as weak pockets, thus promoting the formation of microcracks.

Although the experimental data clearly indicate a decrease in the flexural strength with increasing microencapsulated PCM levels, this is not as pronounced as the decrease observed in compression tests. This is particularly true for 10% and 20% microencapsulated PCM addition, where the reduction of the flexural strength was in the order of 35% and 45%, respectively. The respective decrease in the compressive strength

and the elastic modulus was substantially higher (i.e. 65-86%). Wei, et al. [**59**] have attributed this behavior to the tensile resisting mechanism being more dependent upon failure processes that develop at the matrix-inclusion interfaces, as opposed to compression, where the response is critically affected by the limited strength of the capsules.

The reduction in the mechanical property values noted above is not necessarily a limiting factor for the intended use of the PCM-enhanced mortars hereby considered. According to Ghiassi [**61**], the strength and stiffness of textile-carrying mortars should be compatible with the properties of the substrate being strengthened. This researcher also underlined that TRM systems with effective pseudo ductile response should generally be composed of mortars with elastic moduli several orders of magnitude lower than that of the reinforcement fabric. Taking into account the construction typologies encountered in earthquake-prone regions and the normative requirements for energy and structural upgrading, it is envisaged that the proposed system will more likely have applications on load-bearing and infill masonries [**2**]. Indeed, there is a substantial stock of such structures dating before the introduction of seismic and energy design standards. These are very often composed of brickwork with elastic modulus in the order of 2-4.5 GPa and compressive strength < 8 MPa ([**62**], [**63**], [**64**], [**65**]). It can thus be argued that the mechanical characteristics of the composites containing 10% and 20% microencapsulated PCM are compatible with the quoted brick masonry properties. At the same time, their elastic modulus is close to that of the masonry, hence enabling a more even distribution of stresses between the substrate and the coating overlay. The elastic moduli of the two aforementioned mortars are also significantly lower than that of commonly used reinforcement textiles (typically > 50 GPa for most carbon, glass, basalt, polyphenylene bezobisoxazole and steel fiber fabrics). In fact, the mechanical properties of these composites are directly comparable to those of textile carrying mortars used in other research projects for the retrofitting of masonry elements. For example, Askouni and Papanicolaou [**66**], Basili, et al. [**67**], Giaretton, et al. [**68**], Bertolesi, et al. [**69**] and De Santis, et al. [**70**] report on the successful use of materials with compressive and flexural

strengths in the range of 8.5-22.5 MPa and 3-5.5 MPa, respectively, and with elastic moduli between 3 and 10 GPa.

In terms of damage sensitivity, the previously noted viscoelasticity and crack blunting/deflection effects can mitigate cracking risks according to Wei, et al. [**59**]. Fernandes, et al. [**57**] added that the beneficial influence of such mechanisms reduces the impact of microencapsulated PCM additions on the fracture properties of cementitious materials. This argument is supported by the experimental work of Šavija, et al. [**18**], who successfully incorporated microencapsulated PCMs into engineered cementitious composites exhibiting deflection hardening under flexure. Nevertheless, it is acknowledged that the mechanical performance and fracture characteristics of TRM matrix materials should be considered on a case-by-case basis, taking into account the particular conditions of the intended application and the properties of the substrate to be strengthened.

3.4 Thermal performance

The average values of thermal conductivity, specific heat capacity and thermal diffusivity obtained from dynamic heat transfer measurements are given in Table 5. For 5% microencapsulated PCM addition, a 35% drop in thermal conductivity is noted with respect to the properties of the reference mix design; from ca. 1.7 to 1.1 W/mK. A thermal conductivity close to 0.8 W/mK was recorded for the mixture containing 10% microencapsulated PCM. At 20% PCM addition the thermal conductivity further dropped to 0.6 W/mK. The aforementioned reduction in thermal conductivity agrees well with the literature, whereby the addition of microencapsulated PCMs in cementitious mortars generally leads to a decrease in the value of this property by 10% to 50% (see relevant data in Table 1). This effect is attributed to the less dense microstructure and higher open porosity of microencapsulated PCM-enhanced mortars, compared to the reference mixture. The lower thermal conductivity that the microencapsulated PCM particles possess, in comparison to the polymer modified cementitious matrix and the aggregate particles, also contribute to this effect ([**22**], [**44**], [**45**]). The experimental results are particularly close to corresponding data reported in Jayalath, et al. [**22**] and Ricklefs, et al. [**25**] for cement

mortars. In these studies, the reference compositions had thermal conductivities between 1.5 and 1.7 W/mK, while the incorporation of microencapsulated PCMs as aggregate substitutes at quantities 1%-5% by wt., or as additives at amounts 0.1-0.3 vol./vol., reduced the value of this property by ≤ 1.0 W/mK. Very similar results are found in the study of Cao, et al. [**44**], who tested geopolymer concerte mixtures with microencapsulated PCM dosages from 0% to 3% by wt.

Table 5. Average thermal properties (Coefficient of Variation) at steady state determined from dynamic heat transfer measurements at T= 25 °C and RH = 32% on polymer modified cement mortar samples containing 0% (reference composition), 5%, 10% and 20% PCM. The number of tests reported in each case corresponds to measurements conducted on the same specimen.

Property	No. of tests	Mortar composition			
		0% PCM	5% PCM	10% PCM	20% PCM
Thermal conductivity - λ (W/mK)	3	1.677 (2%)	1.070 (1%)	0.839 (2%)	0.593 (1%)
Specific heat capacity – c_p (J/kgK)	3	883 (1%)	891 (1%)	932 (2%)	1045 (1%)
Thermal diffusivity - a (mm^2/s)	3	1.040 (2%)	0.702 (1%)	0.554 (1%)	0.397 (1%)

The experimental data also show an increase in the specific heat capacity of the PCM-enhanced mortars, which correlates well with their microencapsulated PCM content. The specific heat capacity (883 J/kgK) of the reference composition increases slightly to 891 J/kgK with the addition of 5% microencapsulated PCM. This value rises above 930 J/kgK when the microencapsulated PCM content becomes ≥ 10%. As expected, the composition with 20% microencapsulated PCM exhibits the best thermal energy storage performance, producing a specific heat capacity ca. 1045 J/kgK.

It should be noted that, in the presence of microencapsulated PCMs, specific heat capacity cannot be actually considered as a static property, but is rather temperature-dependent. In fact, differential scanning calorimetry tests performed by Shadnia, et al. [**16**] and Hunger, et al. [**45**] revealed endothermic peaks, when the specific heat capacity varies as a function of temperature. Such peaks occur at the PCM phase transition stage and substantially increase the composite's specific heat capacity when the temperature approaches the PCM's melting point. This is because a considerable amount of heat is used

for changing the state of the PCM inclusion, rather than for raising the temperature of the composite itself. Indeed, additional heat transfer measurements conducted at temperatures above 33 ^{o}C (i.e. after the onset of the selected PCM's phase transition stage) showed that the specific heat capacity of the reference composition remained essentially unaltered, whereas that of the mixtures containing 10% and 20% PCM increased to 958 J/kgK and 1089 J/kgK, respectively. Haurie, et al. [**19**], who tested single layer cementitious mortars at temperatures below the PCM melting point, assessed specific heat capacities of 730 J/kgK for compositions without microencapsulated PCM and 910-920 J/kgK for 10% and 20% microencapsulated PCM addition by wt. of the mixture constituents (including water and powder components); these results are in line with the results obtained in the present study. The aforementioned researchers reported values of specific heat capacity in the range 1160-1260 J/kgK for the same microencapsulated PCM mortars, when the measurements were performed at the liquid phase of the PCM.

Thermal diffusivity is another indicator of thermal inertia, in the sense that materials with lower thermal diffusivity exhibit slower heat conduction rates relative to their volumetric heat storage capacity, and therefore do not respond as quickly to temperature changes. The results hereby obtained verify the positive effect of microencapsulated PCM addition on the thermal diffusivity. The trend recorded is analogous to that noted in the case of thermal conductivity. A thermal diffusivity of 1.040 mm^2/s was measured for the reference mix design. This value decreased by 33% for 5% microencapsulated PCM addition (0.702 mm^2/s). The reduction achieved by 10% and 20% microencapsulated PCM addition was ca. 50%. Other researchers have noted similar results following the testing of cement- [**19**] and lime-based [**37**] microencapsulated PCM-enhanced mortars.

(a)

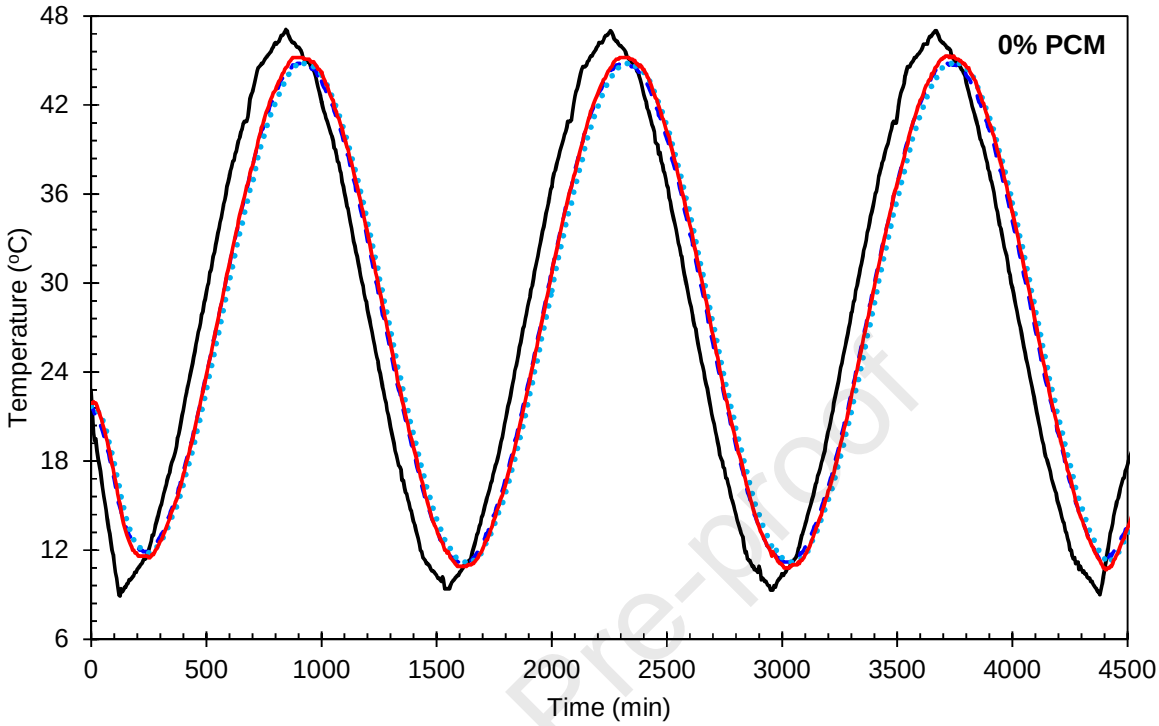

(b)

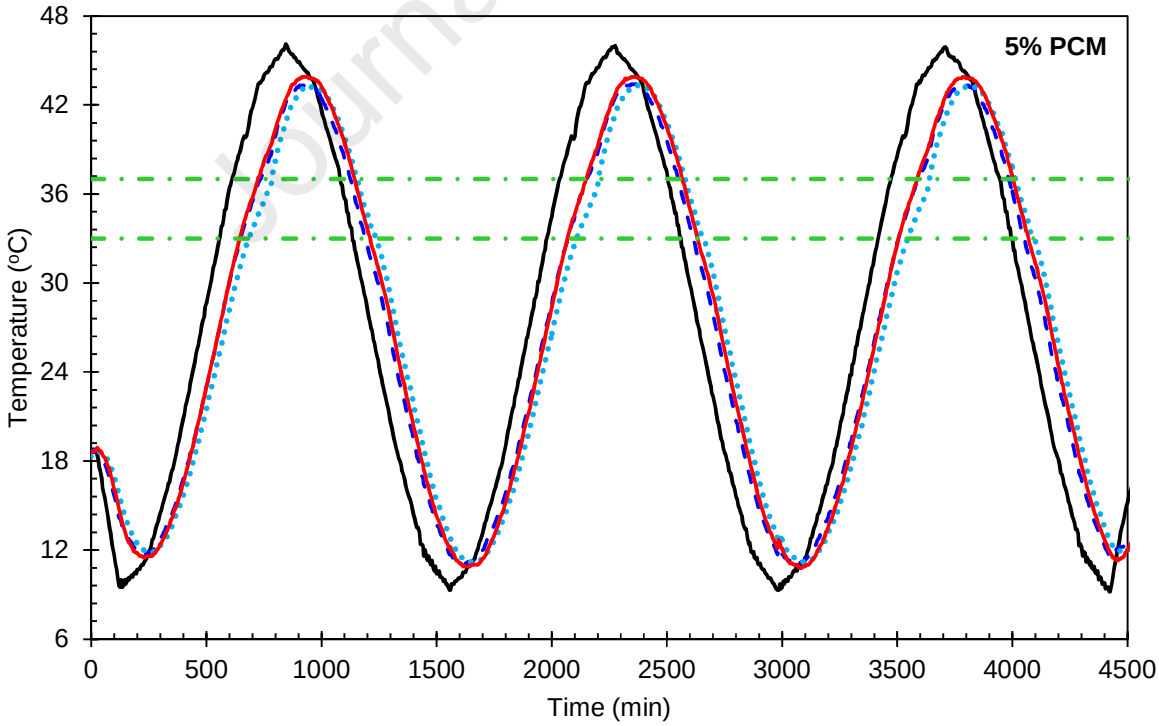

(c)

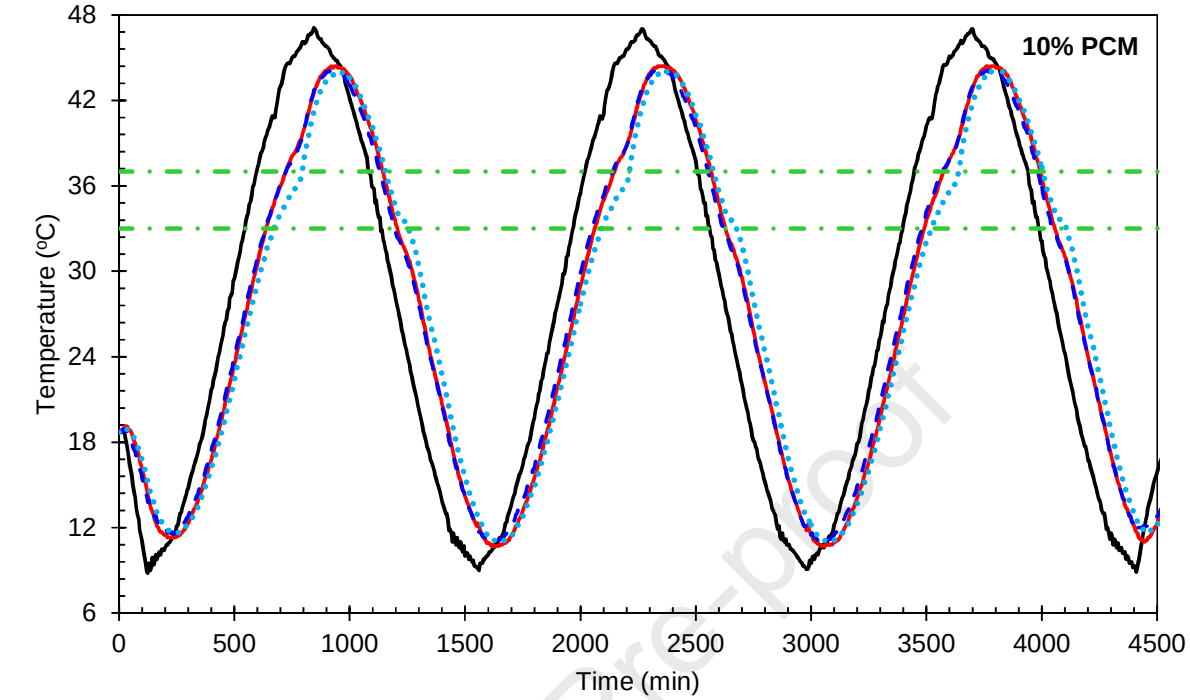

(d)

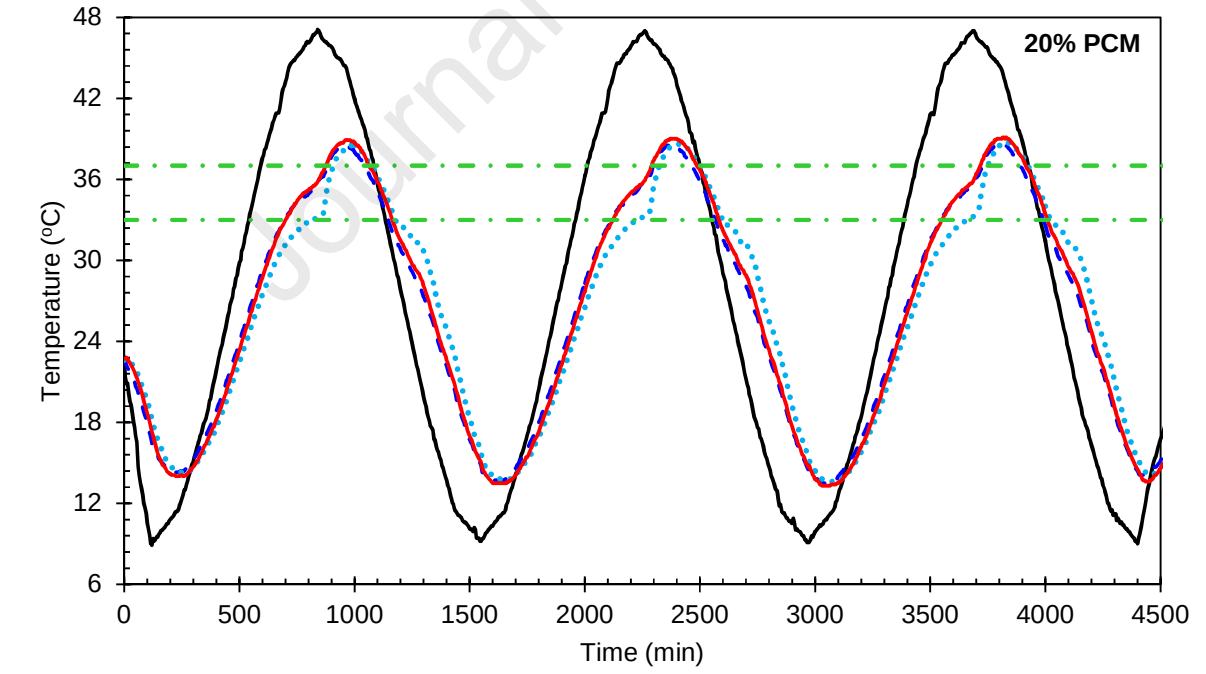

Chamber ambient temperature

Temperature inside the test cell

PCM phase transition temperature range

Mortar exterior surface temperature

Mortar interior surface temperature

Figure 13. Temperature variation over time for mortar specimens containing (a) 0%, (b) 5%, (c) 10% and (d) 20% PCM. The temperatures corresponding to the onset of the phase changing stage and to the melting point of the PCM used are also indicated on the graphs presenting results for PCM-modified mortar mixtures (b-d). Time 0 min corresponds to the time when thermal equilibrium between the test specimens was considered to have been achieved after 24 h exposure to the same ambient temperature (20 ^{o}C).

The experimental data obtained from the climatic chamber tests are presented in Figure 13. A distinct reduction in the rate at which the temperature on the interior surface of the microencapsulated PCM-enhanced mortar plate specimens changes is observed between 33 ^{o}C and 37 ^{o}C. This is clearly due to the melting and re-solidification of the PCM, as the temperature range over which the heating/cooling rate changes coincides with the material's phase transition zone. The scale of this phenomenon is directly linked to the microencapsulated PCM content, and is thus much more noticeable for 20% microencapsulated PCM addition. The same behavior was recorded by Zhang, et al. [**71**], who performed controlled heating experiments on microencapsulated PCM-enhanced cement mortar plates fitted on insulated cubic enclosures.

Comparing the temperatures recorded on the interior surface of the mortar plate samples and at the center of the cubicle enclosures, it is noted that these differ consistently, with the latter being closer to the temperature on the mortars' exterior surface. This is possibly related to heat release within the cubicle by the mortar. In any case, the difference between the ambient exterior temperature and the temperature inside the cubicles is still significant. This is particularly true for the specimens containing 10% and 20% microencapsulated PCM. The same applies for the shifting of thermal peaks. Shadnia, et al. [**16**], who implemented a similar setup to examine the performance of geopolymer mortar plates, reported analogous deviations in the temperatures recorded on the material surfaces and inside the test enclosures.

In order to derive quantitative indicators for the thermal regulating efficiency of the various compositions hereby examined, two additional parameters were computed using the experimental data recorded while subjecting the cubicle test units to temperature variations, namely the decrement factor and the time lag.

The decrement factor represents the reduction in cyclical temperature in relation to the ambient temperature of the exterior environment. It was estimated as:

$$f = \frac{T_{i,max} - T_{i,min}}{T_{e,max} - T_{e,min}} \quad (5)$$

In the above equation $T_{i,max}$ and $T_{i,min}$ are the maximum and minimum temperatures recorded on the interior surface of the mortar plate sample and $T_{e,max}$ and $T_{e,min}$ are the maximum and minimum ambient temperatures recorded at the climatic chamber. It is noted that the latter differ slightly (< 5%) from the respective values (T_{max} = 45.6 ^{o}C and T_{min} = 8.8 ^{o}C) used for programming the chamber's temperature variation due to allowable fluctuations (± 0.4 ^{o}C) in the device's temperature controller system.

The time lag, which represents the time delay due to the thermal mass provided by the mortar plate samples, was estimated as:

$$\Phi = t_{Ti,max} - t_{Te,max} \quad (6)$$

where $t_{Ti,max}$ and $t_{Te,max}$ are the times at which the maximum temperatures at the interior surface of the mortar plate sample ($T_{i,max}$) and in the chamber ($T_{e,max}$) were recorded.

The decrement factor and time lag values were computed for each of the three temperature cycles imposed. The average results are reported in Figure 14. The decrement factors computed indicate that for 5% and 10% microencapsulated PCM addition, the effect posed in terms of moderating temperature fluctuations is rather marginal. However, in comparison to the reference mixture, the 5% and 10% microencapsulated PCM mortars still succeeded in reducing the thermal peaks. The peak temperatures recorded in the chamber and on the interior surface of the plate test specimens differed on an average by 2.2 ^{o}C for the reference composition. The corresponding values recorded for 5% and 10% microencapsulated PCM addition were 2.7 ^{o}C and 3.0 ^{o}C, respectively. A similar influence was not observed at low temperatures. For the compositions with 0%-10% PCM, the temperatures measured at the interior surfaces of the mortar plates were 2.2 ^{o}C higher than the minimum ambient temperature of the chamber. The response of the test sample containing 20% microencapsulated PCM differed subtly. For this composition, the

minimum interior temperature was 4.7 °C higher than that of the chamber, while an impressive 8.4 °C reduction of the peak temperature was also observed. Subsequently, a much lower decrement factor of 0.65 was achieved.

(a)

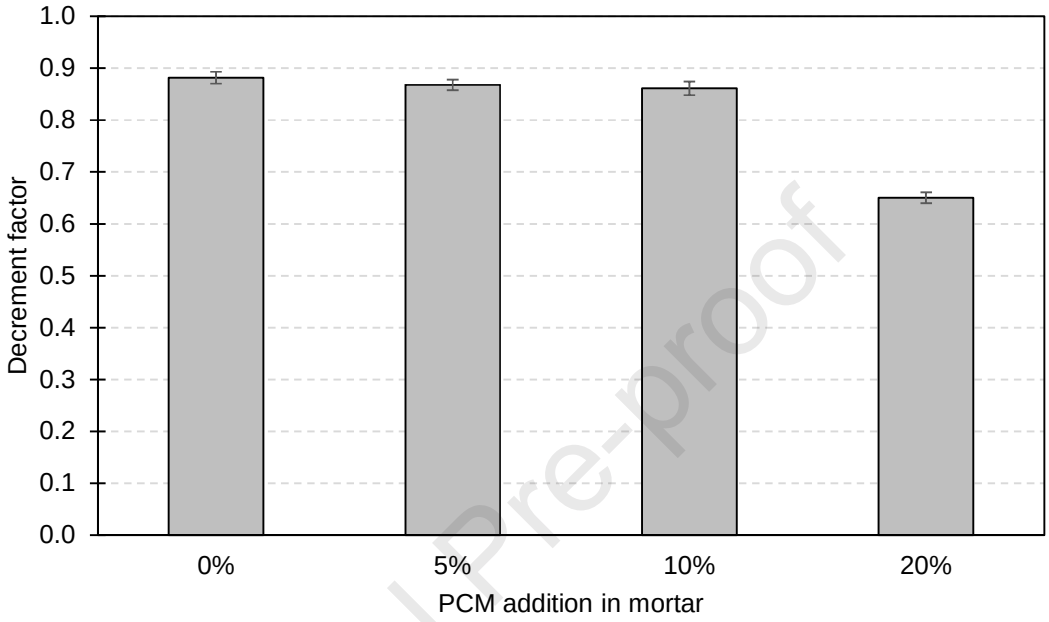

(b)

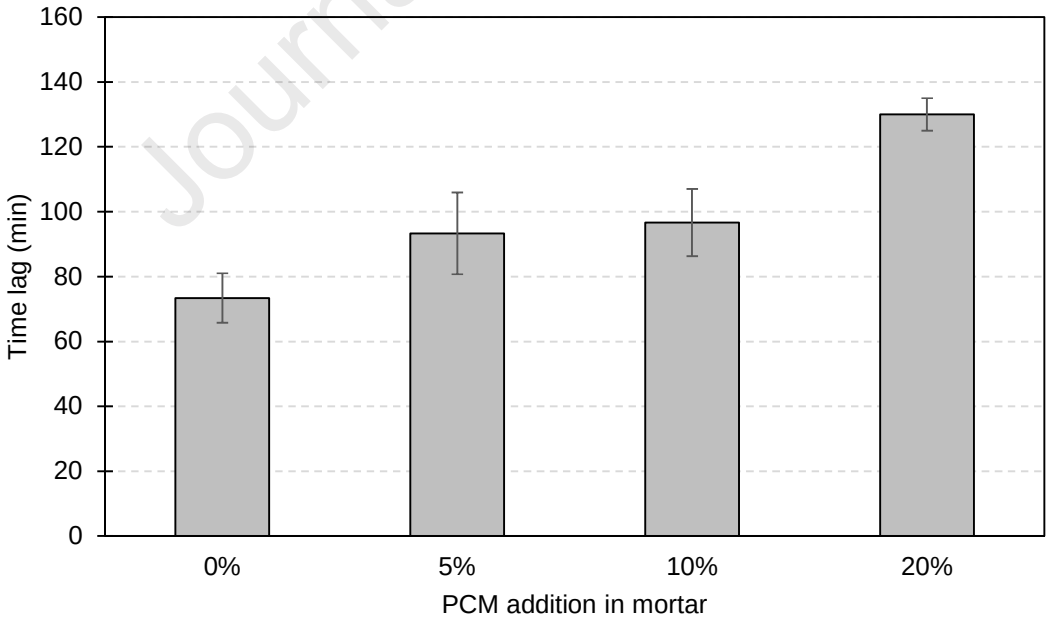

Figure 14. Decrement factor (a) and time lag (b) measured by subjecting the test cubicles to sinusoidal cyclic variations of ambient temperature inside a climatic chamber. The results reported correspond to average values estimated from three test cycles. In each case, deviations between the values obtained from individual test cycles are indicated with error bars.

Of particular interest is the shifting of thermal peaks caused by the addition of microencapsulated PCM. The thermal peaks at the interior surface of the reference mortar occurred 73 min after the time the ambient temperature reached its maximum value. This time increased to approximately 94 min for 5% and 10% microencapsulated PCM content. Again, the mixture containing 20% microencapsulated PCM exhibited the best thermal performance, giving a time lag of 130 min.

Direct comparisons with decrement factors and time lag values reported in the literature are not easy to perform because these parameters are strongly dependent upon the test setup and the specimen dimensions. Nevertheless, some relevant data are quoted for qualitative evaluation purposes. Zhang, et al. [**71**] measured a reduction of peak temperatures near 6 ^{o}C and a time lag of approximately 20 min, when heating up to 40 ^{o}C mortar plates measuring 40 mm in thickness, in which 20% of the cement binder had been replaced by microencapsulated PCM. Cunha, et al. [**20**], who performed cyclic thermal tests with temperature variations 10-45 ^{o}C, observed that microencapsulated PCM incorporation in cement mortars resulted to peak indoor temperatures consistently > 2 ^{o}C lower than the temperatures recorded for conventional mixtures. The time lag in heating conditions also increased from ca. 70 min to 93-104 min. Although these results totally agree with the data hereby obtained, it should be noted that the setup used by Cunha, et al. [**20**] involved the testing of insulated cubic cells, the interior walls of which had been coated with 10 mm thick mortar layers containing 22% microencapsulated PCM by wt. of solid constituents (i.e. 40% by wt. of the sand aggregate). Attenuation of temperature fluctuations by > 2 ^{o}C after the addition of 20% and 30% microencapsulated PCM by wt. of the solid constituents was also reported by Lucas, et al. [**54**], who tested cement mortar samples using the same setup as Cunha, et al. [**20**]. When exposing test cells accommodating geopolymer mortar plates 50 mm thick to outdoor conditions (ambient temperatures 25-50 ^{o}C), Shadnia, et al. [**16**] recorded surface temperatures at the bottom of the specimens containing 2% and 5% microencapsulated PCM by wt. of the solid constituents (i.e. 10% and 20% replacement of sand by vol.) that were 3.3-6.2 ^{o}C lower than those measured for specimens without PCMs. Furthermore, these researchers noticed that the surface temperature started to rise about 70 min later when microencapsulated PCM was used in the mortar mixture. Despite the

different testing conditions encountered in the aforementioned studies, it can be argued that the results reported in the literature fully support the findings presented in this paper regarding the thermal regulating efficiency of microencapsulated PCM-enhanced mortars.

4 Conclusions

The addition of microencapsulated PCMs in polymer modified cement repair mortar was examined in this paper, in the context of developing a composite suitable for the construction of thermally efficient TRM structural overlays for masonry retrofitting. The following conclusions were derived:

- Mixtures containing microencapsulated PCM required higher amounts of water to achieve the desired workability, thus resulting in mortars with a less dense microstructure. This parameter, in combination with the distinct difference between the stiffness and strength of the capsules and the rest of the mortar constituents, are the main factors affecting the physico-mechanical properties of the hardened composites.
- The MIP measurements revealed a shift towards larger pore sizes in the mortars containing microencapsulated PCMs. These results are strongly supported by SEM observations, which showed a noticeable increase in both micro- and macro-porosity with increasing PCM dosage.
- The water absorption due to capillarity was found to deviate from $t^{1/2}$ kinetics. Interestingly, microencapsulated PCM addition at dosages up to 10% did not affect early stage absorption. Although an increase in the initial rate of absorption was noted for 20% microencapsulated PCM addition, the capillary coefficients of all tested mixtures were well below 0.20 kg/m^{2}min$^{1/2}$, which is adequate according to the EN 998-1 specifications for masonry coating mortars.
- In line with the data reported in the literature, a drastic reduction of the compressive and flexural strengths was observed with increasing amounts of microencapsulated

PCMs. Except for the weak nature of the PCM microcapsules themselves and the higher porosity of the PCM-enhanced composites, the reduced mechanical strength recorded could be also attributed to agglomerated PCM particles, which act as weak inclusions under loading. Strength reduction was found to be more profound under compressive loads.

- The influence of microencapsulated PCM addition on the elastic modulus of the mortars hereby tested shows the same trend as that noted for the compressive strength. A significant effect of microencapsulated PCM inclusions on the post-yield compressive hardening repose was observed. Larger microencapsulated PCM dosages increased the deformability of the mortar, thus shifting the strain at the peak compressive stress to higher magnitude.
- Despite the negative influence of microencapsulated PCMs on the mechanical properties of the hardened end-products, all mixtures gave compressive and flexural strengths above 10 MPa and 4 MPa, respectively, and elastic moduli > 4 GPa. The aforementioned values may be perceived as thresholds, based on existing literature regarding TRMs. Mortars containing 10% and 20% microencapsulated PCM were also found to possess mechanical properties compatible with clay brick masonry.
- Dynamic heat transfer measurements showed a decrease in thermal conductivity with microencapsulated PCM content. At the same time, an increase in the specific heat capacity and a reduction of the thermal diffusivity were observed. This indicates the beneficial effect of microencapsulated PCM addition on the thermal mass and thermal inertia of the mortars hereby studied.
- Climatic chamber tests on cubicles, carried out at conditions resembling local spring-summer diurnal temperature fluctuations, showed that a ca. 3 ^{o}C reduction of the peak indoor temperature can be attained by mortars containing 5%-10% microencapsulated PCMs. These samples also succeeded in shifting the thermal peaks by approximately 95 min. An impressive attenuation in cyclical temperature variations was recorded in the case of the mixture with 20% microencapsulated PCMs, which gave a decrement factor of 0.65 and a time lag of 130 min.

Based on the aforementioned results, it can be concluded that the incorporation of microencapsulated PCMs in textile-carrying polymer mortars is feasible. For the particular materials examined in this study, microencapsulated PCM dosages > 5% and ≤ 20% w/w are deemed to be appropriate for achieving favorable thermal performance, without compromising the physico-mechanical behavior of the end-product. It should be highlighted that the selection of the appropriate dosage of PCM is essentially an optimization problem, for which different parameters need to be accounted for [**72**]. For the proposed type of application, the amount of microencapsulated PCM addition should be selected on a case-by-case basis. The ultimate goal should be adequate thermal and physico-mechanical properties of the composite, depending on the specific characteristics of the substrate to be retrofitted and the local climatic conditions.

Acknowledgements

The work presented in this paper has been undertaken in the framework of the research project "*Novel integrated approach for seismic and energy upgrading of existing buildings*" (INTEGRATED/0916/0004), which is co-funded by the Cyprus Research and Innovation Foundation and the European Regional Development Fund, under the Integrated Projects call of the "RESTART 2016-2020" Programme for Research, Technological Development and Innovation. The authors would also like to acknowledge Loucas Kyriakou for his help with the MIP tests.

Data Availability

The raw/processed data required to reproduce these findings cannot be shared at this time as the data also forms part of an ongoing study.

References

[1] EU 2018/844. Directive (EU) 2018/844 of the European Parliament and of the Council of 30 May 2018 amending Directive 2010/31/EU on the energy performance of buildings and Directive 2012/27/EU on energy efficiency. Official Journal of the European Union. 2018;L 156(75).

[2] Bournas DA. Concurrent seismic and energy retrofitting of RC and masonry building envelopes using inorganic textile-based composites combined with insulation materials: A new concept. Composites Part B: Engineering. 2018;148:166-179.

[3] Triantafillou TC, Karlos K, Kefalou K, Argyropoulou E. An innovative structural and energy retrofitting system for URM walls using textile reinforced mortars combined with thermal insulation: Mechanical and fire behavior. Construction and Building Materials. 2017;133:1-13.

[4] Koutas LN, Tetta Z, Bournas DA, Triantafillou TC. Strengthening of Concrete Structures with Textile Reinforced Mortars: State-of-the-Art Review. Journal of Composites for Construction. 2019;23(1):https://doi.org/10.1061/(ASCE)CC.1943-5614.0000882.

[5] Baetens R, Jelle BP, Gustavsen A. Phase change materials for building applications: A state-of-the-art review. Energy and Buildings. 2010;42(9):1361-1368.

[6] Demirbas MF. Thermal Energy Storage and Phase Change Materials: An Overview. Energy Sources, Part B: Economics, Planning, and Policy. 2006;1(1):85-95.

[7] Farid MM, Khudhair AM, Razack SAK, Al-Hallaj S. A review on phase change energy storage: materials and applications. Energy Conversion and Management. 2004;45:1597-1615.

[8] Tatsidjodoung P, Le Pierrès N, Luo L. A review of potential materials for thermal energy storage in building applications. Renewable and Sustainable Energy Reviews. 2013;18:327-349.

[9] Cui Y, Xie J, Liu J, Pan S. Review of Phase Change Materials Integrated in Building Walls for Energy Saving. Procedia Engineering. 2015b;121:763-770.

[10] Venkateswara Rao V, Parameshwaran R, Vinayaka Ram V. PCM-mortar based construction materials for energy efficient buildings: A review on research trends. Energy and Buildings. 2018;158:95-122.

[11] Konuklu Y, Ostry M, Paksoy HO, Charvat P. Review on using microencapsulated phase change materials (PCM) in building applications. Energy and Buildings. 2015;106:134-155.

[12] Alva G, Lin Y, Liu L, Fang G. Synthesis, characterization and applications of microencapsulated phase change materials in thermal energy storage: A review. Energy and Buildings. 2017;144:276-294.

[13] Peng G, Dou G, Hu Y, Sun Y, Chen Z. Phase Change Material (PCM) Microcapsules for Thermal Energy Storage. Advances in Polymer Technology. 2020;2020:https://doi.org/10.1155/2020/9490873.

[14] Sanfelix SG, Santacruz I, Szczotok AM, Bello LMO, De la Torre AG, Kjøniksen AL. Effect of microencapsulated phase change materials on the flow behavior of cement composites. Construction

and Building Materials. 2019;202:353-362.

[15] Kheradmand M, Abdollahnejad Z, Pacheco-Torgal F. Alkali-activated cement-based binder mortars containing phase change materials (PCMs): mechanical properties and cost analysis. European Journal of Environmental and Civil Engineering. 2018 https://doi.org/10.1080/19648189.2018.1446362.

[16] Shadnia R, Zhang L, Li P. Experimental study of geopolymer mortar with incorporated PCM. Construction and Building Materials. 2015;84:95-102.

[17] Aguayo M, Das S, Maroli A, Kabay N, Mertens JCE, Rajan SD, Sant G, Chawla N, Neithalat N. The influence of microencapsulated phase change material (PCM) characteristics on the microstructure and strength of cementitious composites: Experiments and finite element simulations. Cement and Concrete Composites. 2016;73:29-41.

[18] Šavija B, Luković M, Kotteman GMG, Figuieredo SC, Filho FFM, Schlangen E. Development of ductile cementitious composites incorporating microencapsulated phase change materials. International Journal of Advances in Engineering Sciences and Applied Mathematics. 2017b;9:169-180.

[19] Haurie L, Serrano S, Boscha M, Fernandez AI, Cabeza LF. Single layer mortars with microencapsulated PCM: Study of physical and thermal properties, and fire behaviour. Energy and Buildings. 2016;111:393-400.

[20] Cunha S, Aguiar J, Ferreira V. Eco-efficient mortars with incorporation of phase change materials. Journal of Building Physics. 2018;41(5):469-492.

[21] Cunha S, Aguiar J, Ferreira V, Tadeu A. Mortars based in different binders with incorporation of phase-change materials: Physical and mechanical properties. European Journal of Environmental and Civil Engineering. 2015a;19(10):1216-1233.

[22] Jayalath A, San Nicolas R, Sofi M, Shanks R, Ngo T, Aye L, Priyan M. Properties of cementitious mortar and concrete containing micro-encapsulated phase change materials. Construction and Building Materials. 2016;120:408-417.

[23] Lecompte T, Le Bideau P, Glouannec P, Nortershauser D, Le Masson S. Mechanical and thermo-physical behaviour of concretes and mortars containing phase change material. Energy and Buildings. 2015;94:52-60.

[24] Joulin A, Zalewski L, Lassue S, Naji H. Experimental investigation of thermal characteristics of a mortar with or without a micro-encapsulated phase change material. Applied Thermal Engineering. 2014;66:171-180.

[25] Ricklefs A, Thiele AM, Falzone G, Sant G, Pilon L. Thermal conductivity of cementitious composites containing microencapsulated phase change materials. International Journal of Heat and Mass Transfer. 2017;104:71-82.

[26] Guardia C, Barluenga G, Palomar I, Diarce G. Thermal enhanced cement-lime mortars with phase change materials (PCM), lightweight aggregate and cellulose fibers. Construction and Building Materials. 2019;221:586-594.

[27] EN 1504-3. Products and systems for the protection and repair of concrete structures. Definitions, requirements, quality control and evaluation of conformity. Structural and non-structural repair. Brussels: CEN; 2005.

[28] EN 12190. Products and systems for the protection and repair of concrete structures. Test methods. Determination of compressive strength of repair mortar. Brussels: CEN; 1999.

[29] EN 1015-3. Methods of test for mortar for masonry. - Part 3: Determination of consistence of fresh mortar (by flow table). Brussels: CEN; 1999.

[30] Coppola L, Coffetti D, Lorenzi S. Cement-Based Renders Manufactured with Phase-Change Materials: Applications and Feasibility. Advances in Materials Science and Engineering. 2016;2016:1-6.

[31] Hall C, Hoff WD. Water Transport in Brick, Stone and Concrete. 2nd ed. Boca Raton: CRC Press; 2012.

[32] EN 1015-18. Methods of test for mortar for masonry. - Part 18: Determination of water absorption coefficient due to capillary action of hardened mortar. Brussels : CEN; 2002.

[33] EN 1015-11. Methods of test for mortar for masonry - Part 11: Determination of flexural and compressive strentgth of hardened mortar. Brussels: CEN; 1999.

[34] EN 13412. Products and systems for the protection and repair of concrete structures. Test methods. Determination of modulus of elasticity in compression. Brussels: CEN; 2006.

[35] Pavlík Z, Trník A, Keppert M, Pavlíková M, Žumár J, Černý R. Experimental Investigation of the Properties of Lime-Based Plaster-Containing PCM for Enhancing the Heat-Storage Capacity of Building Envelopes. International Journal of Thermophysics. 2013;35:767-782.

[36] Siwińska A, Garbalińska H. Thermal conductivity coefficient of cement-based mortars as air relative humidity function. Heat Mass Transfer. 2011;47:1077-1087.

[37] Theodoridou M, Kyriakou L, Ioannou I. PCM-enhanced Lime Plasters for Vernacular and Contemporary Architecture. Energy Procedia. 2016;97:539-545.

[38] ASTM D 5334. Standard Test Method for Determination of Thermal Conductivity of Soil and Soft Rock by Thermal Needle Probe Procedure. West Conshohocken, PA: ASTM International, www.astm.org; 2008.

[39] Young BA, Falzone G, Wei Z, Sant G, Pilon L. Reduced-scale experiments to evaluate performance of composite building envelopes containing phase change materials. Construction and Building Materials. 2018;162:584-595.

[40] Ramakrishnana S, Wang X, Sanjayan J, Wilson J. Thermal energy storage enhancement of lightweight cement mortars with the application of phase change materials. Procedia Engineering. 2017;180:1170-1177.

[41] Djamai ZI, Salvatore F, Larbi AS, Cai G, El Mankibi M. Multiphysics analysis of effects of encapsulated phase change materials (PCMs) in cement mortars. Cement and Concrete Research. 2019;119:51-63.

[42] Nepomuceno MCS, Silva PD. Experimental evaluation of cement mortars with phase change material incorporated via lightweight expanded clay aggregate. Construction and Building Materials. 2014;63:89-96.

[43] Djamai ZI, Larbi AS, Salvatore F, Cai G. A new PCM-TRC composite: A mechanical and physicochemical investigation. Cement and Concrete Research. 2020;153:106-119.

[44] Cao VD, Pilehvar S, Salas-Bringas C, Szczotok AM, Rodriguez JF, Carmona M, Al-Manasir N, Kjøniksen AL. Microencapsulated phase change materials for enhancing the thermal performance of Portland cement concrete and geopolymer concrete for passive building applications. Energy Conversion and Management. 2017;133:56-66.

[45] Hunger M, Entrop AG, Mandilaras I, Brouwers HJH, Founti M. The behavior of self-compacting concrete containing micro-encapsulated Phase Change Materials. Cement & Concrete Composites. 2009;31:731-743.

[46] Cao VD, Pilehvar S, Salas-Bringas C, Szczotok AM, Bui TQ, Carmona M, Rodriguez JF, Kjøniksen AL. Thermal performance and numerical simulation of geopolymer concrete containing different types of thermoregulating materials for passive building applications. Energy and Buildings. 2018;173:678-688.

[47] Cui H, Liao W, Memon SA, Dong B, Tang W. Thermophysical and Mechanical Properties of Hardened Cement Paste with Microencapsulated Phase Change Materials for Energy Storage. Materials (Basel). 2014;7(12):8070-8087.

[48] Eddhahak A, Drissi S, Colin J, Caré S, Neji J. Effect of phase change materials on the hydration reaction and kinetic of PCM-mortars. Journal of Thermal Analysis and Calorimetry. 2014;117:537-545.

[49] EN 998-1. Specification for mortar for masonry. Rendering and plastering mortar. Brussels: CEN; 2016.

[50] Hall C, Raymond Yau MH. Water movement in porous building materials-IX. The water absorption and sorptivity of concretes. Building and Environment. 1987;22(1):77-82.

[51] Ioannou I, Hamilton H, Hall C. Capillary absorption of water and n-decane by autoclaved aerated concrete. Cement and Concrete Research. 2008a;38:766-771.

[52] Ioannou I, Hall C, Hamilton A. Application of the Sharp Front Model to capillary absorption in concrete materials with bimodal pore size distribution. In: International RILEM Symposium on Concrete Modelling; 2008b; Delft, 26-28 May. p. 521-525.

[53] Pilehvar S, Cao VD, Szczotok AM, Valentini L, Salvioni D, Magistri M, Pamies R, Kjøniksen AL. Mechanical properties and microscale changes of geopolymer concrete and Portland cement concrete containing micro-encapsulated phase change materials. Cement and Concrete Research. 2017;100:341-349.

[54] Lucas SS, Ferreira VM, de Aguiar JLB. Latent heat storage in PCM containing mortars—Study of microstructural modifications. Energy and Buildings. 2013;66:724-731.

[55] Harsh S, Shen Z, Darwin D. Strain-Rate Sensitive Behavior of Cement Paste and Mortar in Compression. ACI Materials Journal. 1990;87(5):508-516.

[56] Falzone G, Falla GP, Wei Z, Zhao M, Kumar A, Bauchy M, Neithalath N, Pilon L, Santa S. The influences of soft and stiff inclusions on the mechanical properties of cementitious composites. Cement and Concrete Composites. 2016;71:153-165.

[57] Fernandes F, Manari S, Aguayo M, Santos K, Oey T, Wei Z, Falzone G, Neithalath N, Sant G. On the feasibility of using phase change materials (PCMs) to mitigate thermal cracking in cementitious materials. Cement and Concrete Composites. 2014;51:14-26.

[58] Xu W, Jia M, Zhu Z, Liu M, Lei D, Gou X. n-Phase micromechanical framework for the conductivity and elastic modulus of particulate composites: Design to microencapsulated phase change materials (MPCMs)-cementitious composites. Materials & Design. 2018;145:108-115.

[59] Wei Z, Falzone G, Das S, Saklani N, Le Pape Y, Pilon L, Neithalath N, Santa G. Restrained shrinkage cracking of cementitious composites containing soft PCM inclusions: A paste (matrix) controlled response. Materials & Design. 2017;132:367-374.

[60] Das S, Maroli A, Neithalath N. Finite element-based micromechanical modeling of the influence of phase properties on the elastic response of cementitious mortars. Construction and Building Materials. 2016;127:153-166.

[61] Ghiassi B. Mechanics and durability of textile reinforced mortars: a review of recent advances and open issues. RILEM Technical Letters. 2019;4:130-137.

[62] Singh SB, Munjal P. Bond strength and compressive stress-strain characteristics of brick masonry. Journal of Building Engineering. 2017;9:10-16.

[63] Radovanović Ž, Grebović RS, Dimovska S, Serdar N, Vatin N, Murgul V. Testing of the Mechanical Properties of Masonry Walls - Determination of Compressive Strength. Applied Mechanics and Materials. 2015;725-726:410-418.

[64] Segura J, Pelà L, Roca P. Monotonic and cyclic testing of clay brick and lime mortar masonry in compression. Construction and Building Materials. 2018;193:453-466.

[65] Kaushik HB, Rai DC, Jain SK. Stress-Strain Characteristics of Clay Brick Masonry under Uniaxial Compression. Journal of Materials in Civil Engineering. 2007;19(9):728-739.

[66] Askouni PD, Papanicolaou CG. Textile Reinforced Mortar-to-masonry bond: Experimental investigation of bond-critical parameters. Construction and Building Materials. 2019;207:535-547.

[67] Basili M, Vestroni F, Marcari G. Brick masonry panels strengthened with textile reinforced mortar: experimentation and numerical analysis. Construction and Building Materials. 2019;227:1-15.

[68] Giaretton M, Dizhur D, Garbin E, Ingham JM. In-Plane Strengthening of Clay Brick and Block Masonry Walls Using Textile-Reinforced Mortar. Journal of Composites for Construction. 2018;22(5):1-10.

[69] Bertolesi E, Buitrago M, Giordano E, Calderón PA, Moragues JJ, Clementi F, Adam JM. Effectiveness of textile reinforced mortar (TRM) materials in preventing seismic-induced damage in a U-shaped masonry structure submitted to pseudo-dynamic excitations. Construction and Building Materials. 2020;248:https://doi.org/10.1016/j.conbuildmat.2020.118532.

[70] De Santis S, de Felice G, Roscini F. Retrofitting of Masonry Vaults by Basalt Textile-Reinforced Mortar Overlays. International Journal of Architectural Heritage. 2019;13(7):1061-1077.

[71] Zhang H, Xing F, Cui HZ, Chen DZ, Ouyang X, Xu SZ, Wang JX, Huang YT, Zuo JD, Tang JN. A novel phase-change cement composite for thermal energy storage: Fabrication, thermal and mechanical properties. Applied Energy. 2016;170:130-139.

[72] Cai R, Sun Z, Yu H, Meng E, Wang J, Dai M. Review on optimization of phase change parameters in phase change material building envelopes. Journal of Building Engineering. 2020;https://doi.org/10.1016/j.jobe.2020.101979.

Highlights

- Microencapsulated Phase Change Materials (PCMs) added in polymeric cement mortar.
- Study of microstructure, physico-mechanical and thermal properties of the mortar.
- Porosity increased, while strength dropped with increasing PCM dosage.
- PCMs contributed to the attenuation and time shifting of temperature peaks.
- Incorporation of PCMs (up to 20% w/w) in textile-carrying mortars is feasible.

Declaration of interests

☒ The authors declare that they have no known competing financial interests or personal relationships that could have appeared to influence the work reported in this paper.

☐The authors declare the following financial interests/personal relationships which may be considered as potential competing interests: